学位の種類	博士（薬科学）
報告番号	甲第１６４６号
学位記番号	第３２９号
氏名	SHAIMAA MOHAMED RAMADAN ELABD IBRAHIM
授与年月日	平成 30 年 3 月 26 日
学位論文の題名	Development of nanomedicines as drug delivery systems for cancer and malaria parasites
論文審査担当者	主査：　湯浅 博昭 副査：　尾関 哲也，牧野 利明，平嶋 尚英

名古屋市立大学学位論文

Development of nanomedicines as drug delivery systems for cancer and malaria parasites

平成 29 年度（西暦 2018 年 3 月）

名古屋市立大学大学院薬学研究科
博士後期課程創薬機能科学専攻
薬物送達学分野

SHAIMAA MOHAMED RAMADAN ELABD IBRAHIM

本論文は、2018 年 3 月名古屋市立大学大学院薬学研究科において審査されたものである。

主査　湯浅　博昭　教　授
副査　尾関　哲也　教　授
　　平嶋　尚英　教　授
　　牧野　利明　教　授

本論文は、学術情報雑誌に収載された次の報文を基礎とするものである。

1. Ibrahim S, Tagami T, Ozeki T: Effective-Loading of Platinum-Chloroquine into PEGylated Neutral and Cationic Liposomes as a Drug Delivery System for Resistant Malaria Parasites. Biol. Pharm. Bull. 40, 813-823 (2017).

2. Ibrahim S, Tagami T, Kishi T, Ozeki T: Curcumin marinosomes as promising nano drug delivery formulation for lung cancer. Int. J. Pharm. 540, 40–49 (2018).

本論文の基礎となる研究は、尾関　哲也教授の指導の下に名古屋市立大学大学院薬学研究科において行われた。

Table of contents

Abstract

One of the most important applications of nanotechnology is the drug delivery system that aims to develop nanomedicines able to deliver the therapeutic compounds into the diseased organ. The formulation and evaluation of drug delivery systems for example liposomes and lipid nanoparticis is less expensive than developing new drugs and can fulfill the objective of increasing the therapeutic activity and decreasing the toxic side effects.

This thesis has three chapters. In the first chapter, we introduced a brief background on nanotechnology and drug delivery, liposomes as drug delivery systems, nonomedicine against malaria and nonomedicine against cancer. In this chapter, we also discussed the importance of using drug delivery nanomedicines to fight infectious diseases like malaria and serious diseases as cancer.

In the second chapter, a liposomal nano drug delivery formulation was prepared to face resistant malaria parasites. The trans platinum-chloroquine diphosphate dichloride (PtCQ) is a new type of antimalarial drug used to fight parasites resistant to traditional drugs. PtCQ is synthesized by mixing platinum and chloroquine diphosphate (CQ). This study examines two efficient methods for forming a nanodrug, PtCQ-loaded liposomes, for use as a potential antimalarial drug-delivery system: the thin drug-lipid film method to incorporate the drug into a liposomal membrane, and a remote-loading method to load the drug into the interior of a cationic liposome. The membranes accordingly comprised PEGylated (contain polyethylene glycol (PEG) polymer) neutral or cationic liposomes. PtCQ was efficiently loaded into PEGylated neutral and cationic liposomes using the thin drug-lipid film method (encapsulation efficiency, EE: 76.1 ± 6.7% for neutral liposomes, 1:14 drug-to-lipid weight ratio; 70.4 ± 9.8% for cationic liposomes, 1:14 drug-to-lipid weight ratio. More PtCQ was loaded into PEGylated neutral liposomes using the remote-loading method than by the thin

drug-lipid film method and the EE was maximum (96.1 ± 4.5 % for neutral liposomes, 1:7 (w/w)). PtCQ was encapsulated in PEGylated cationic liposomes comprising various amounts of cationic lipids (0-20 mol%; EE: 96.9-92.3%) using the remote-loading method. PEGylated neutral liposomes and cationic liposomes exhibited minimum leakage of PtCQ after two months' storage at 4˚C, and further exhibited little release under in vitro culture conditions at 37˚C for 72 hours. These results provide a useful framework for the design of future liposome-based in vivo drug delivery systems targeting the malaria parasite.

In the third chapter, a marinosomal nano drug delivery formulation was prepared to face lung cancer, which considered as the major cause of cancer-related death worldwide. Curcumin attracted attention due to its promising anti-cancer properties, however its poor aqueous solubility and bioavailability have to be overcome. In the current study curcumin is encapsulated in krill lipids-based liposomes (marinosomes) to develop a potential anticancer therapy from low-cost and readily available nutraceuticals. Reflux followed by thin drug-lipid film method is used successfully to incorporate the drug into the liposomal membrane at high encapsulation efficiency (EE). The curcumin-loaded marinosomes (CURMs) showed a powerful antioxidant activity (EC_{50}: 4.1 ± 0.3 μg/mL). Additionally, CURMs exhibited high physicochemical and oxidative stability after eight weeks' storage at 4˚C. Furthermore, CURMs exhibited sustained release of about 30 % of their curcumin content under in vitro culture conditions at 37˚C after 72 hrs. Consequently, CURMs showed its maximum cytotoxic effect (IC_{50}; 11.7 ± 0.24 μg/ml) after incubation for 72 hrs against adenocarcinomic human alveolar basal (A549) cells. Additionally, CURMs inhibited the proliferation of human umbilical vein endothelial cells (HUVECs) in a dose-dependent manner with IC_{50} of 2.5 ± 2.1 μg/ml. The current study presents the CURM as a favorable in vitro drug delivery system to target cancer disease.

CHAPTER 1

Introduction and objectives

1.1. Background

1.1.1 Nanotechnology and drug delivery

From being a relatively small field to a worldwide scientific and industrial field, nanotechnology has been sprung in the last decades. One of the aims of nanotechnology is the development of functional materials, devices and systems in the nanometer scale. The biological functions depend mainly on the nanoscale dimensions of the cellular components where these functions take place (Li et al., 2017). Consequently, nanomaterials are similar in size to these biologic molecules and small enough to interact with and deliver to them. One of the most important applications of nanotechnology is the drug delivery system that aims to develop nanomedicines able to deliver the therapeutic compounds into the diseased organ (Shi et al., 2010). Therefore, drug delivery system is able to improve the solubility of hydrophobic drugs, reduce the potential immunogenicity, release the drugs in a sustained release phenomenom, increase the therapeutic activity and decrease the toxic side effects. Different biodegradable materials, including natural or synthetic polymers, lipids, or metals were used in preparation of nanoparticles and used as drug delivery systems (Suri et al., 2007). These drug delivery systems were generally < 100 nm and taken up by cells more efficiently while the drug can either be integrated in the matrix of the particle or attached to the particle surface. To

control the drug entering into the biological environment, nano drug delivery targeting systems with different compositions and biological properties have been plentifully investigated for drug and gene delivery applications (Pison et al., 2006; Schatzlein et al., 2006; Brannon-Peppase et al., 2004; Yokoyama et al., 2005; Stylios et al., 2005).

1.1.2 Liposomes as drug delivery systems

Colloidal drug delivery systems such as liposomes, micelles or nanoparticles have been plentifully investigated for using in cancer therapy, shown in **Fig. 1**. The first description of swollen phospholipid systems has been reported in 1965 and followed by establishing the basis for model membrane systems (Bangham et al., 1965; Papahadjopoulos et al., 1967; Bangham et al., 1967). Bangosomes, which are enclosed phospholipid bilayer structures consisting of single bilayer, were the initial term of liposomes that described later (Deamer et al., 2010; Batzri et al., 1973). liposomes cabability to entrap drugs and to be used as drug delivery systems is a concept that is established by Gregory Gregoriadis (Gregoriadis et al., 1971; Gregoriadis et al., 1973). Later, the cabability of liposomes to change the in vivo distribution of entrapped drugs has been investigated (Kimelberg et al., 1976; Poste et al., 1976). Extrusion of multilamellar vesicles through polycarbonate membranes to produce large unilamellar vesicles (LUV) with defined size distribution was a particularly important advance (Olson et al., 1979). Sonication or homogenization was later used to produce “limit size” LUV with diameters less than 50 nm (Huang et al., 1969). However, a scalable

production of LUV in the 20–50 nm size range was produced using microfluidic-mixing approaches (Zhigaltsev et al., 2012).

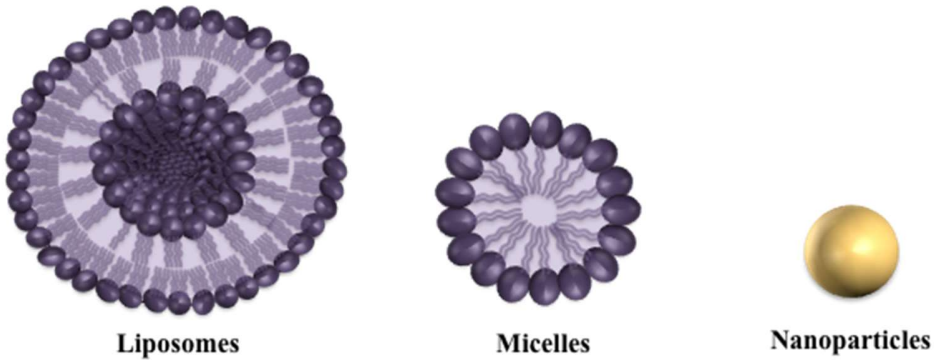

Fig. 1 Schematic representation of some colloidal drug delivery systems

1.1.3 Nonomedicine against malaria

Malaria is a life-threatening infectious disease that remains a major cause of death, caused by a parasitic protozoan, *Plasmodium falciparum*, and is transmitted by infected *Anopheles* mosquitoes. People living in the poorest countries are the most vulnerable, with approximately 80 % of deaths in Africa (World Malaria Report, 2015). The life cycle of *Plasmodium* parasites involves the injection of malaria parasite into the bloodstream (Greenwood et al., 2008; Miller et al., 2013). The parasite grows and divides in the erythrocytes by absorbing the nutrients from the blood.

Most current antimalarial drugs distribute widely into body tissues and metabolized easily in the liver after systemic or oral administration because they are

amphiphilic (Greenwood et al., 2008). Consequently, a high dose that may cause toxic side effects is needed to provide a therapeutic effect. Lowering the dose to avoid toxicity lead to the development of resistance. Therefore, there is therefore an urgent need to develop new strategies to treat malaria and overcome the resistance of the parasite to current antimalarial drugs. These new strategies are including the formulation of novel delivery systems. The formulation and evaluation of drug delivery systems is less expensive than developing new drugs and can fulfill the objective of increasing drug bioavailability and thus increasing the therapeutic activity, decreasing side effects due to reduced dosing and increased selectivity of the drugs. Consequently, lipid nanoparticles such as liposomal formulations that encapsulate antimalarial drugs have been developed over the past years in order to test their utility in the treatment of malaria (Urbán et al., 2011; Moles et al., 2015; Peeters et al., 1989; Santos-Magalhães et al., 2010).

1.1.4 Nonomedicine against lung cancer

Cancer is a major cause of morbidity and mortality, which affecting populations in all countries with approximately 14 million new cases and 8 million cancer-related deaths in 2012 as estimated by the international Agency for Research on Cancer (GLOBOCAN, 2012). Generally, the high-resource countries (North America, western Europe, Japan, Korea, Australia, and New Zealand) were found to have the highest incidence of cancer. The lowest incidence rates are seen in Africa and West and South Asia. Similar world maps of the estimated global age-standardized mortality rates. In contrast, the less economically developed countries show more cancer deaths for a given number of

incident cases, and cancer mortality rates are not very different from those in more developed countries. This could be due to clinical care, improved cancer survival and the good prognosis of cancers associated with a lifestyle of developed countries (Soerjomataram et al., 2015).

Surgery, radiation, and chemotherapy are considered to be the conventional cancer therapies for cancer. Surgery has the incidence of operative mortality or postoperative complications. Radiation and chemotherapy may result in a lot of negative side effects including renal, neurologic, aplasia, pneumonitis and pericarditis toxic effects. Additionally, the hydrophobicity of most of chemotherapeutic drugs, which leads to poor aquous solubility and low bioavailability, with the lack of selectivity for the cancer cells result in the development of multidrug resistance (Chidambaram et al., 2011). In order to maximize tumor control and minimize chemotherapy side effects, potential alternatives and non-toxic therapies for lung cancer have to be continuing investigated. Nanotherapeutics is a rapidly progressing field of cancer research and able to solve the above-mentioned side effects of conventional chemotherapy. Nanotechnology provides nanoparticles that are able to increase the drug solubility, bioavailability and deliver chemotherapies directly and specifically to cancer cells in order to decrease or eliminate the toxic side effects.

1.2. Objectives

The objective of this study is facing infectious diseases as malaria and serious diseases like cancer using nanotechnology. One of the most important applications of nanotechnology is the drug delivery system that aims to develop nanomedicines able to deliver the therapeutic compounds into the diseased organ. The formulation and evaluation of drug delivery systems for example liposomes and lipid nanoparticis is less expensive than developing new drugs and can fulfill the objective of:

1- Improving the solubility of hydrophobic drugs
2- Increasing the encapsulation efficiency
3- Releasing the drugs in a sustained release phenomenon.
4- Increasing the therapeutic activity
5- Decreasing the toxic side effects
6- Decreasing the cost

In the current study, two nano drug delivery systems were developed and characterized. One is for malaria, which is among the biggest killer diseases in the developing world. Platinum Chloroquine Diphosphate Dichloride complex (PtCQ) showed therapeutic effects againt chloroquine resistant malaria parasites. However and for the first time to encapsulate PtCQ into cationic liposomes with high encapsulation efficiency and high stability using remote loading method employing ammonium sulfate gradient. These PtCQ cationic liposomes hold promise for the future treatment of malaria and serious diseases. The other nano drug delivery system is for cancer, which is among

the leading killers in the developed countries. To the best of our knowledge, it is the first time to use krill lipid based liposomes to encapsulate a highly hydrophobic compound to prepare a low cost controlled drug delivery medicine to target cancer and other inflammatory diseases. These curcumin-loaded marinosomes exhibit high encapsulation efficiency, high antioxidant activity, and high physicochemical and oxidative stability. These curcumin-loaded marinosomes exhibited an effective cytotoxic effect on lung cancer (A549) and HUVEC cells. Hope these two drug delivery systems to be two feathers in the wings of the healing bird that fly on both worlds.

1.3. References

Bangham, A.D., Standish, M.M., Watkins, J.C., 1965. Diffusion of univalent ions across the lamellae of swollen phospholipids. J. Mol. Biol 13, 238–252.

Bangham, A.D., Standish, M.M., Watkins, J.C., Weissmann, G., 1967. The diffusion of ions from a phospholipid model membrane system. Protoplasma 63, 183–187.

Batzri, S., Korn, E.D., 1973. Single bilayer liposomes prepared without sonication. Biochim. Biophys. Acta. 16, 1015–1019.

Brannon-Peppase, L., Blanchette, J.Q., 2004. Nanoparticle and targeted systems for cancer therapy. Adv. Drug. Deliv. Rev. 56, 1649–1659.

Deamer, D.W., 2010. From "banghasomes" to liposomes: a memoir of Alec Bangham, 1921–2010, FASEB. J 24, 1308–1310.

Ferlay, J., Soerjomataram, I., Dikshit, R. 2015. Cancer incidence and mortality worldwide: sources, methods and major patterns in GLOBOCAN 2012. Int. J. Cancer 136, E359–E386.

GLOBOCAN: Global Burden of Cancer Study. Agency for Research on Cancer (2012).

Greenwood, B.M., Fidock, D.A., Kyle, D.E., Kappe, S.H., Alonso, P.L., Collins, P.L.F.H., P. E. Duffy, P.E., 2008. Malaria: progress, perils, and prospects for eradication. J. Clin. Invest. 118, 1266–1276.

Gregoriadis, G., Ryman, B.E., 1971. Liposomes as carriers of enzymes or drugs: a new approach to the treatment of storage diseases. Biochem. J. 124, 58P.

Gregoriadis, G., 1973. Drug entrapment in liposomes. FEBS. Lett. 36, 292–296.

Huang, C., 1969. Studies on phosphatidylcholine vesicles: formation and physical characteristics. Biochemistry 8, 344–352

Kimelberg, H.K., Tracy, T.F., Biddlecome, S.M., Bourke, R.S., 1976. The effect of entrap-ment in liposomes on the in vivo distribution of H-methotrexate in a primate. Cancer Res. 36, 2949–2957.

Li, Y., Zhang, D., Capoglu, I., Hujsak, K.A., Damania, D., Cherkezyan, L., Roth, E., Bleher, R., Wu, J.S., Subramanian, H., Dravid, V.P., Backman, V., 2017. Measuring the autocorrelation function of nanoscale three-dimensional density distribution in individual cells using scanning transmission electron microscopy, atomic force microscopy, and a new deconvolution algorithm. Microsc. Microanal. 23, 661–667.

Miller, L.H., Ackermen, H.C., Su, X-Z, Wellems, T.E., 2013. Malaria biology and disease pathogenesis: insights for new treatments. Nature Med. 19, 156–167.

Moles, E., Urbán, P., Jiménez-Díaz, M.B., Viera-Morilla, S., Angulo-Barturen, I., Busquets, M.A., Fernàndez-Busquets, X., 2015. Immunoliposome-mediated drug delivery to *Plasmodium*-infected and non-infected red blood cells as a dual therapeutic/prophylactic antimalarial strategy. J. Control. Release. 210, 217–229.

Olson, F., Hunt, C.A., Szoka, F.C., Vail, W.J., Papahadjopoulos, D., 1979. Preparation of liposomes of defined size distribution by extrusion through polycarbonate membranes. Biochim. Biophys. Acta 557, 9–23.

Papahadjopoulos, D., Watkins, J.C., 1967. Phospholipid model membranes. II. Permeability properties of hydrated liquid crystals, Biochim. Biophys. Acta. 135, 639–652.

Peeters, P.A.M., Huiskamp, C.W.E.M., Eling, W.M.C. and Crommelin, D.J.A, 1989. Chloroquine containing liposomes in the chemotherapy of murine malaria. Cambridge J., Parasitol. 98, 381–386.

Pison, U., Welte, T., Giersig, M., and Groneberg, D.A., 2006. Nanomedicine for respiratory diseases. Eur. J. Pharmacol. 533, 341–350.

Poste, G., Papahadjopoulos, D., 1976. Lipid vesicles as carriers for introducing materials into cultured cells: influence of vesicle lipid composition on mechanism(s) of vesicle incorporation into cells. Proc. Natl. Acad. Sci. U.S.A. 73, 1603–1607.

Santos-Magalhães, N. S., Mosqueira, V. C. F, 2010. Nanotechnology applied to the treatment of malaria. Adv. Drug Deliv. Rev. 62, 560–575.

Schatzlein, A.G., 2006. Delivering cancer stem cell therapies – A role for nanomedicines? Eur. J. Cancer 42, 1309–1315.

Shi, J., Votruba, A.R., Farokhzad O.C., and Langer, R., 2010. Nanotechnology in drug delivery and tissue engineering: from discovery to applications. Nano Aalett 10, 3223–3230.

Stylios, G.K., Giannoudis, P.V., and Wan, T., 2005. Applications of nanotechnologies in medical practice. Injury 36, S6–S13.

Suri, S.S., Fenniri, H., Singh, B., 2007. Nanotechnology-based drug delivery systems, J. Occup. Med. Toxicol. 1, 2–16.

Urbán, P., Estelrich, J., Cortés, A., Fernàndez-Busquets, X., 2011. A nanovector with complete discrimination for targeted delivery to *Plasmodium falciparum*-infected versus non-infected red blood cells in vitro. J. Control. Release. 151, 202–211.

WHO: World Malaria Report. World Health Organization (2015).

Yokoyama. M., 2005. Drug targeting with nano-sized carrier systems. J. Artif. Organs 8, 77–84.

Zhigaltsev, I. V., Belliveau, N., Hafez, I., Leung, A.K., Huft, J., Hansen, C., Cullis, P.R., 2012. Bottom-up design and synthesis of limit size lipid nanoparticle systems with aqueous and triglyceride cores using millisecond microfluidic mixing. Langmuir 28, 3633–3640.

CHAPTER 2

Effective loading of platinum–chloroquine into PEGylated neutral and cationic liposomes as a drug delivery system for resistant malaria parasites

2.1. Introduction

Malaria is a life-threatening infectious disease that remains a major cause of death, especially in tropical regions. The WHO estimated that 214 million new cases of malaria resulted in 438000 deaths in 2015 (WHO, 2015). The mortality rate of malaria is higher than that caused by AIDS. Malaria is caused by a parasitic protozoan, *Plasmodium falciparum*, and is transmitted by infected Anopheles mosquitoes. The life cycle of *Plasmodium* parasites involves being bitten by an infected mosquito, during which the malaria parasite is injected into the bloodstream (Greenwood et al., 2008; Miller et al., 2013). The parasite migrates into hepatocytes and establishes itself in the liver. After a few weeks of dormancy, the activated parasite enters the blood and then infiltrates erythrocytes (red blood cells; RBCs). The parasite grows and divides in the erythrocytes by absorbing the nutrients from the blood via transporters, and these transporters are currently a topic of investigation by medical researchers.

The amphiphilicity of most current antimalarial drugs lead them to distribute widely into body tissues after systemic or oral administration, and can be easily

metabolized in the liver (Greenwood et al., 2008), and thus a high dose that may cause toxic side effects is needed to provide an antimalarial effect. The need to lower the dose to avoid toxicity is likely a main factor contributing to the development of resistance; this low dose also means that an ineffective dose is delivered to *Plasmodium*-infected RBCs. There is therefore an urgent need to develop new strategies to treat malaria and overcome the resistance of the parasite to current antimalarial drugs, especially in regions where *Plasmodium falciparum* is endemic.

Lipid-based drug nano-carriers have various advantages for drug delivery (Baruah et al., 2017). For example, liposomal formulations can increase drug bioavailability and thus increase therapeutic activity, decreasing side effects due to reduced dosing. *Plasmodium*-infected RBCs are the main chemotherapeutic target because several life stages of the parasite occur in the blood and give rise to the symptoms and pathologies of malaria. Consequently, several liposomal formulations encapsulating antimalarial drugs have been developed over the past several years in order to test their utility in malaria chemotherapy (Peeters et al., 1989; Santos-Magalhães et al., 2010). Additionally, immunoliposomes have been widely investigated and showed significant therapeutic effects (Urbán et al., 2011; Moles et al., 2015). However, one of the most drawbacks of immunoliposomes is that the antigens from different subspecies of malarial parasites are different. Therefore novel and universal drug delivery systems, which have effective targeting ability against various kinds of malaria parasites have been pursuing.

CHAPTER 2: Effective loading of platinum–chloroquine into PEGylated neutral and cationic liposomes as a drug delivery system for resistant malaria parasites

---

The ability of cationic liposomes to be adsorbed onto the cell surface and fuse with the negatively charged cellular membranes and thus deliver their cargo has been previously reported and shown in **Fig. 2** (Li et al., 1997; Stebelska et al., 2006; Obata et al., 2010; Campbell et al., 2009; Zhao et al., 2011; Abu Lila et al., 2009). Anionic lipids such as phosphatidylserine (PS) are typically located within the inner monolayer of erythrocytes. The infection of erythrocytes with the malaria parasite leads to erythrocyte apoptosis, and this suicidal erythrocyte death is called eryptosis. The main characteristic stage of eryptosis is lipid scrambling and exposure of negatively charged PS on the outer surface of erythrocytes (Tagami et al., 2015; Föller et al., 2009), which increase the ability of erythrocytes to fuse with cationic liposomes (Stebelska et al., 2006). However, the use of cationic liposomes in vivo is limited due to their short circulation time, which leads to their recognition by the immune system including macrophages (Levchenko et al., 2002; Johnstone et al., 2001; Campbell et al., 2002). It is well known that polyethylene glycol (PEG) prevents the interaction with the biological in vivo environment and extend the circulation time of liposomes in blood. Cationic liposomes are therefore promising candidates for drug delivery targeting malaria-infected RBCs, but currently there is little information regarding the use of cationic liposomes. Additionally, cationic liposomes have not applied yet towards a working strategy for the treatment of malaria.

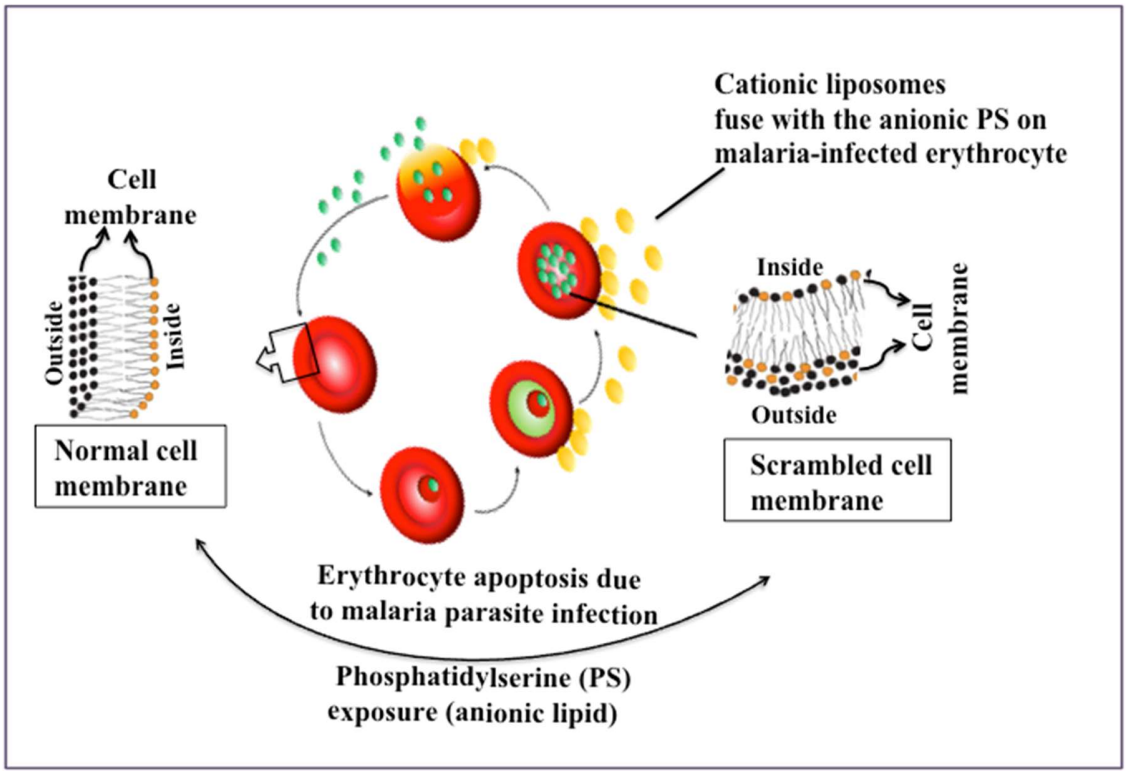

Fig. 2 Targeting of malaria-infected erythrocytes by cationic liposomes

Cationic liposomes have the ability to fuse with the negatively charged cellular membranes and thus deliver its cargo.

CHAPTER 2: Effective loading of platinum–chloroquine into PEGylated neutral and cationic liposomes as a drug delivery system for resistant malaria parasites

Hemoglobin catabolism is an essential process that provides the parasite with amino acids it needs to grow resulting in the formation of heme. For Energy production purpose, the parasite converts heme into hematin. As hematin is toxic, the parasite converts it into hemozoin, which is chemically identical to β-hematin. The mechanism of action of chloroquine (CQ) is based on the inhibition of detoxification of hematin products by the parasite through interaction with hematin and preventing the formation of hemozoin causing the parasite to be poisoned by its own metabolic products. Although promising were the CQ antimalrial effects, the emergence and spread of CQ-resistant parasites is a growing global health problem (Navarro et al., 2011; Urbán et al., 2011). PtCQ is a trans platinum-chloroquine complex that shows therapeutic effects against the chloroquine-resistant malaria parasite. The high lipophilicity of PtCQ and the structural modification of CQ imposed by the presence of Plattinum lead to enhanced activity and ability to lower CQ resistance. Consequently, the main mechanism of anti-malarial action of PtCQ was the interaction of this metal compound with the specific target ferriprotoporphyrin IX (Fe (III) PPIX) and inhibition of β-haematinin in order to increase anti-malarial activity and fight the parasite resistance (Navarro et al., 2011).

The present study focuses on generating PtCQ-loaded PEGylated cationic liposomes exhibiting high drug encapsulation and high drug retention. Foremost, many fundamental properties of PtCQ, such as drug solubility, remain poorly investigated, although it was reported that PtCQ dissolves in dimethylsulphoxide (DMSO). We therefore investigated methods for efficiently loading PtCQ into liposomes and first

characterized the handling properties of PtCQ. Next; PtCQ was loaded with high encapsulation efficiency into cationic liposomes for the first time using the remote-loading method employing an ammonium sulfate gradient as shown in **Fig. 3**. The liposome formulations showed good drug retention, minimum leakage of PtCQ after two months' storage at 4˚C, and further exhibited little release under in vitro culture conditions at 37˚C for 72 hours.

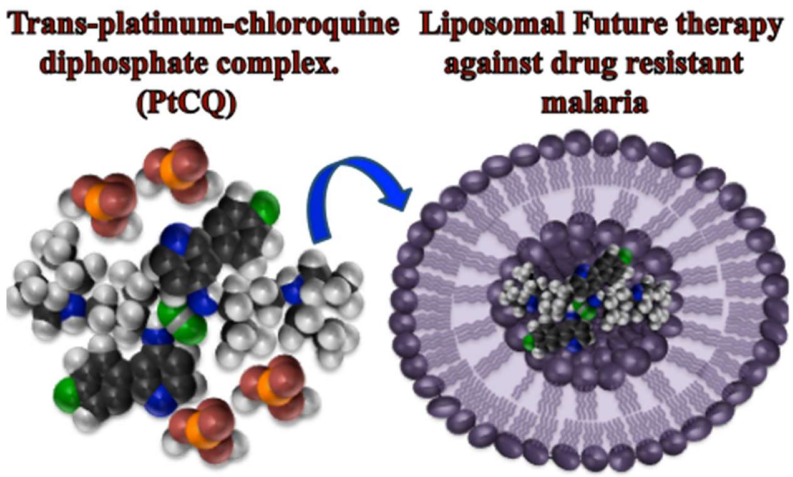

Fig. 3 The efficient drug encapsulation into PEGylated cationic liposomes by using remote-loading method

2.2. Materials and Methods

2.2.1 Reagents

Chloroquine diphosphate (CQDP), potassium tetrachloroplatinate ($K_2[PtCl_4]$), hydrogenated soy phosphatidylcholine (HSPC), 1,2-dioleoyl-3-trimethylammonium-propane (DOTAP) and cholesterol (CHOL) were purchased from Wako Pure Chemical Industries, Ltd. (Osaka, Japan). 1,2-Distearoyl-*sn*-glycero-3-phosphoethanolamine-*N*-[methoxy (polyethylene glycol)-2000] (DSPE-PEG_{2000}) was generously donated by NOF Corporation (Tokyo, Japan).

2.2.2 Synthesis of the trans-$Pt(CQDP)_2(Cl)_2$ complex (Navarro et al., 2011)

The trans-$Pt(CQDP)_2(Cl)_2$ complex was synthesized as shown in **Fig. 4**. A solution of $K_2[PtCl_4]$ (100 mg, 0.24 mmol) in water (30 ml) was stirred until it completely dissolved and then CQDP (250 mg, 0.48 mmol) was added. Stirring was continued for 18 hours at room temperature and a pink precipitate was obtained. This precipitate was collected by filtration, washed with water, and dried under vacuum.

Yield 87.8% (calculated as in **Fig. 5**); elemental analysis (%) Calc. for $C_{36}H_{64}N_6Cl_4O_{16}P_4Pt$ (1297.65 $g.mol^{-1}$): C 33.3; N 6.5; H 4.9. Found: C 31.7; N 6.7; H 4.4. IR υ (N-H) 3305 cm^{-1}; υ (C=C) 1616 cm^{-1}; υ (C=N) 1581 cm^{-1}; υ (Pt-cl) 341 cm^{-1}; υ (Pt-N) 420 cm^{-1}. UV-vis 238 and 344 nm. ^{1}H-NMR (DMSO-d6; δ ppm): 9.05 (1H; d; J, 6.09 Hz; NH); 8.82 (1H; d; J, 9.13 Hz; H5); 8.58 (1H; d; J, 7.01 Hz; H2); 8.02 (1H; d; J, 1.83 Hz; H8); 7.8 (1H; dd; J1, 1.83 and J2, 7.01 Hz; H6); 7.02 (1H; d; J, 7.01 Hz; H3);

4.17 (1H; m; H1′); 3.15 (6H, m, H4′ and H5′); 1.79 (4H; m; H2′ and H3′); 1.3 (3H; d; J, 6.39 Hz; H1′′); 1.18 (6H, t, H6′).

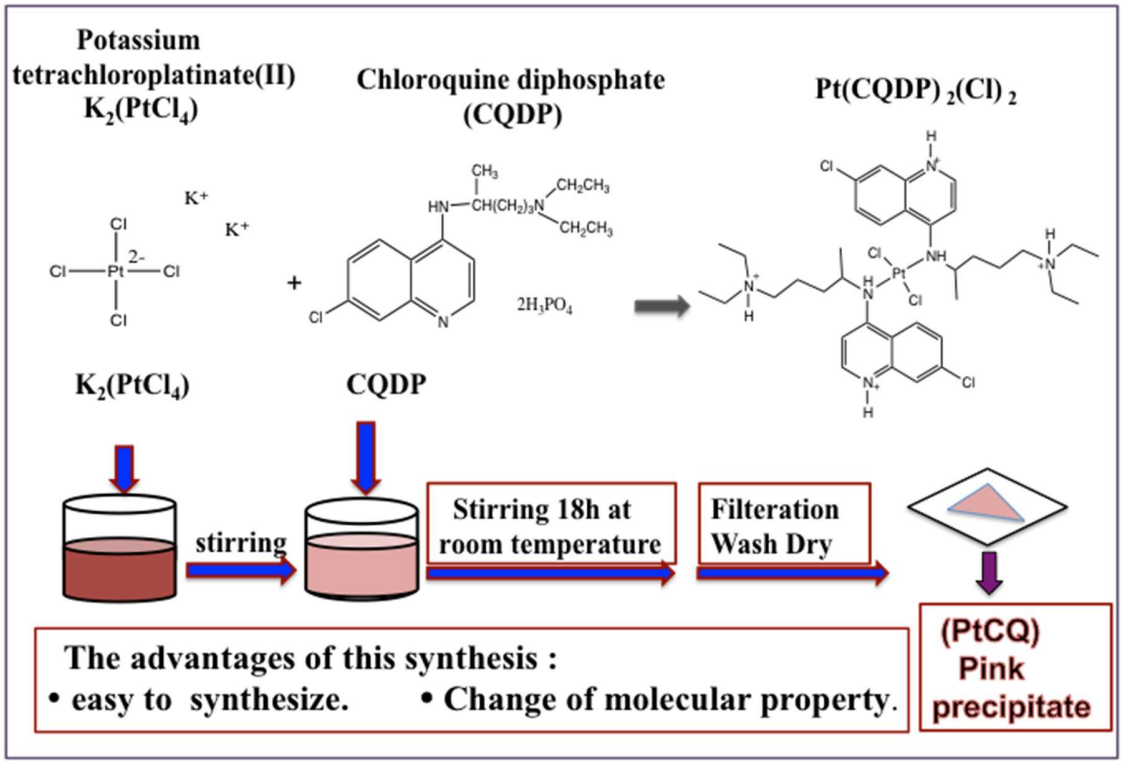

Fig. 4 Synthesis of platinum chloroquine diphosphate dichloride (PtCQ)

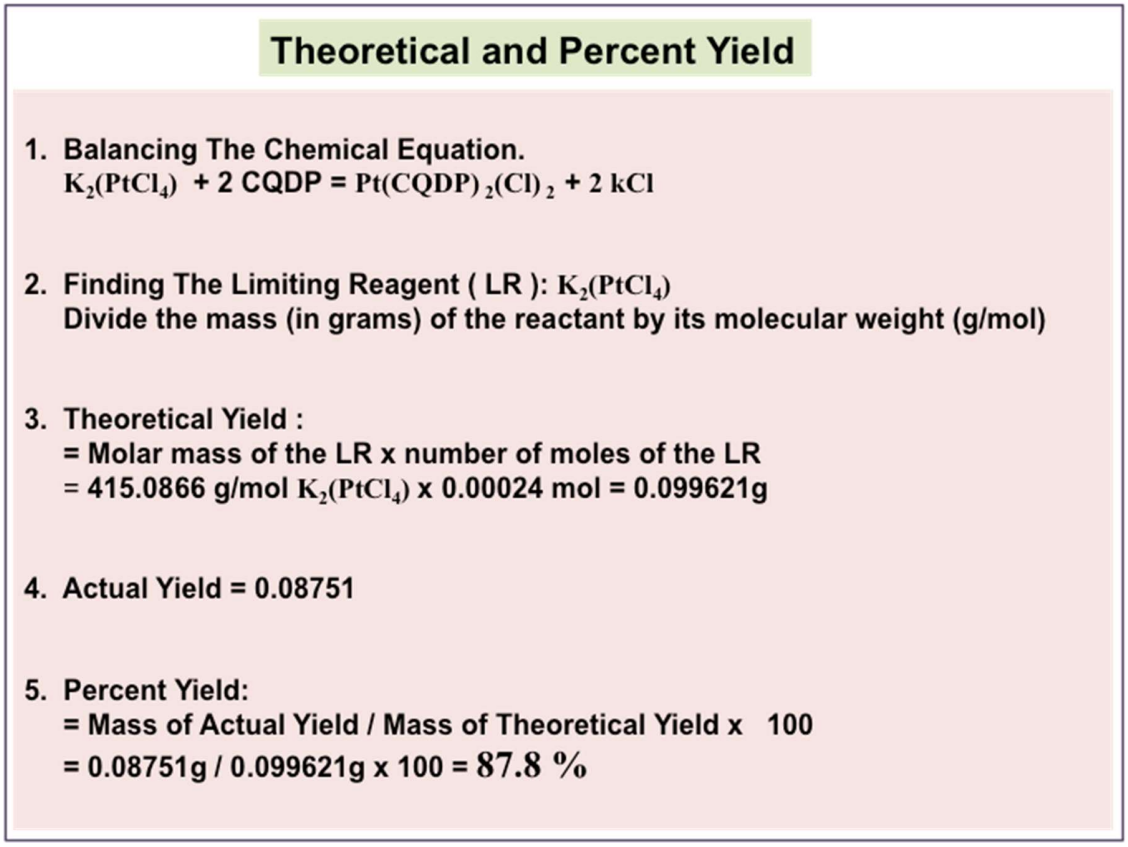

Fig. 5 Theoretical and percent yield

2.2.3 Preparation of PtCQ-loaded liposomes using the thin drug-lipid film method

Liposomes were prepared by the thin drug-lipid film hydration method, followed by membrane extrusion as shown in **Fig. 6** and described previously, with minor modifications (Isacchi1 et al., 2011). Briefly, neutral PtCQ-loaded liposomes were prepared by dissolving each lipid powder (HSPC, CHOL and DSPE-PEG$_{2000}$) with isopropanol and mixed at the molar ratio 55:45:5 (HSPC: CHOL: DSPE-PEG$_{2000}$). PtCQ (1 mg) was dissolved in dichloromethane (DCM) and a trace of DMSO (The details in **Fig. 7** and **Fig. 8**) and then added to the lipid mixture. The drug-lipid mixture was evaporated to give a thin drug-lipid film that was placed under high vacuum for at least overnight to remove residual solvent. The dried drug-lipid film was hydrated in HBS (20 mM HEPES, 150 mM NaCl, pH 7.5) to form multilamellar vesicles (MLVs), sonicated for 10 min, and then extruded (Mini-extruder, Avanti Polar Lipids, Alabaster, AL, USA) 10 times through Whatman Nuclepore Track-Etched polycarbonate membranes (GE Healthcare Life Sciences; Chicago, IL, USA) with 200 nm pores and then with 100 nm pores at 70˚C to transform the MLVs into unilamellar vesicles. The formulation was cooled on ice for 15 min and unencapsulated PtCQ was removed by ultracentrifugation (2.1×10^4 g, 4˚C, 30 min) as previously reported (Laouini et al., 2012). Cationic PtCQ-loaded liposomes were prepared by dissolving the lipids (HSPC: DOTAP: CHOL: DSPE-PEG$_{2000}$) in isopropanol, then mixing in the molar ratio 50:5:45:5, and 35:20:45:5. PtCQ (1 mg) was added to the lipid mixture at different weight ratios (1:7, 1:14) and then the vesicles were prepared as described above. The mean size and polydispersity index

(PDI) were determined using a dynamic light scattering instrument (ZetaSizer Nano-ZS; Malvern Instrument Ltd., Malvern, U.K). Zeta potentials were measured using Zetasizer Nano ZS90 (Malvern). The zeta potentials were measured by dispersing the liposome solution in 5% dextrose. The encapsulation efficiency (EE) was calculated as described in "Determination of the EE."

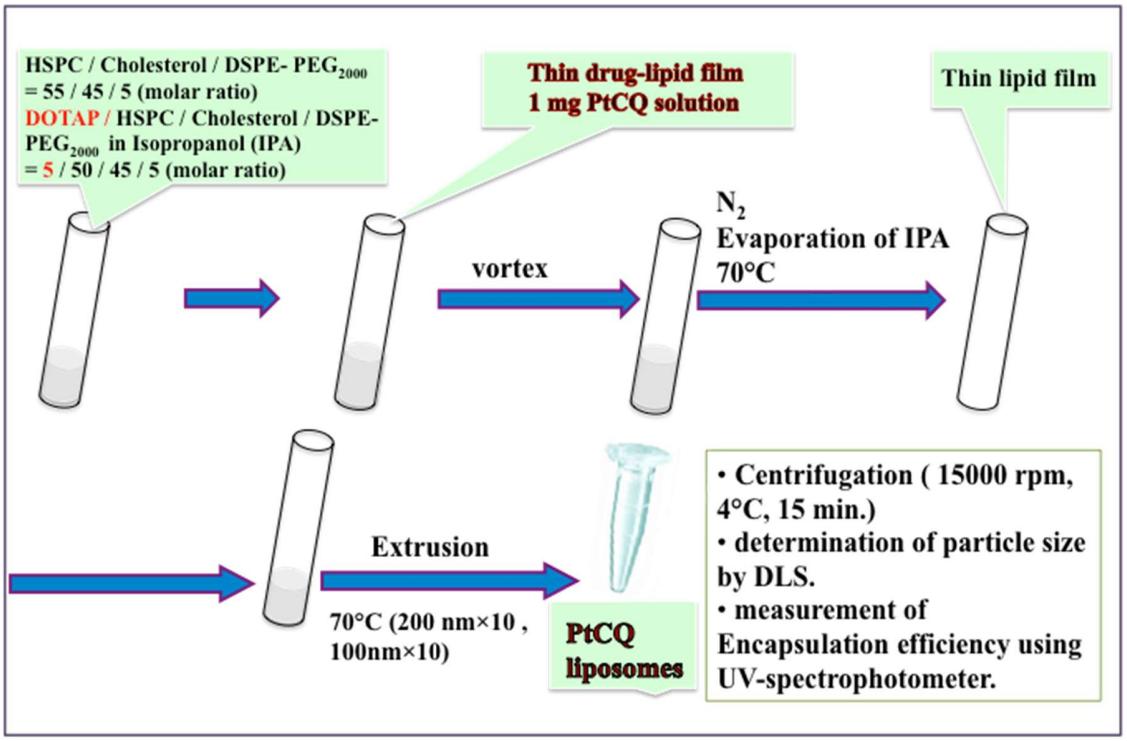

Fig. 6 Preparation of PtCQ-liposomes by thin drug-lipid film

Fig. 7 Fundamental properties of PtCQ

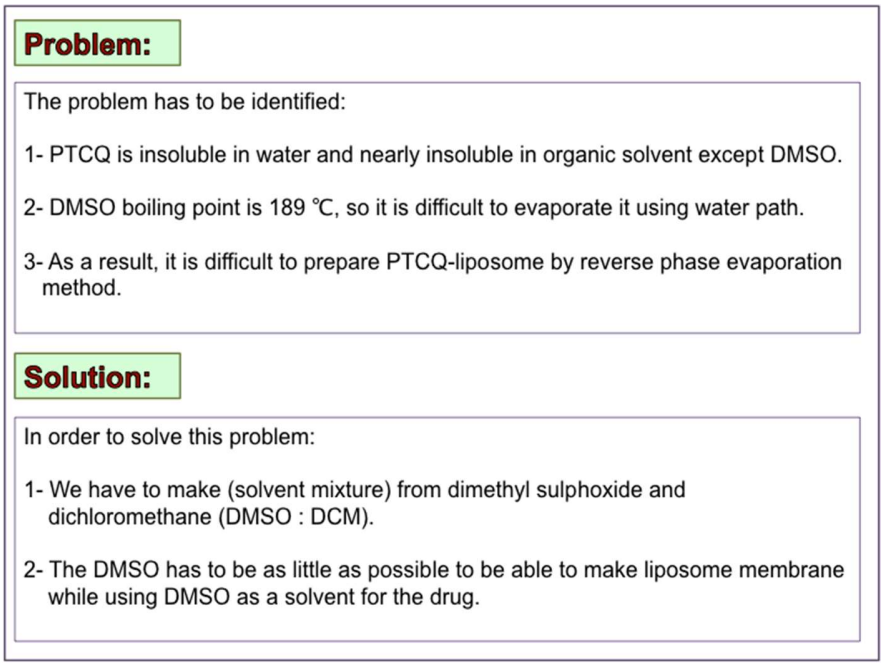

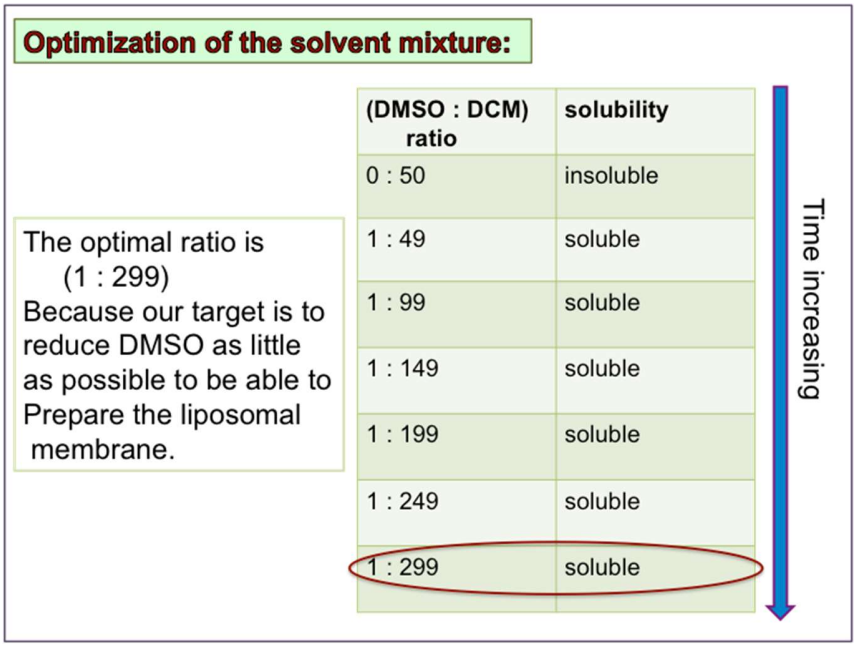

Fig. 8 Optimal ratio of DMSO and DCM

2.2.4 Preparation of PtCQ-loaded liposomes using the remote-loading method

PtCQ-loaded liposomes were prepared as as shown in **Fig. 9** and previously reported, with minor modifications (Haran et al., 1993; Tagami et al., 2015; Tagami et al., 2014; Qiu et al., 2008). Briefly, neutral PtCQ-loaded liposomes were prepared by mixing the lipids (HSPC: CHOL: DSPE-PEG$_{2000}$) at the molar ratio 55:45:5. Cationic PtCQ-loaded liposomes were prepared by mixing the lipids (HSPC: DOTAP: CHOL: DSPE-PEG$_{2000}$) with different molar ratios of the cationic lipid DOTAP (0, 5, 10, 15 and 20 mol%) and dissolving in organic solvent. The solvent from the lipid mixtures was evaporated to provide thin lipid films that were placed under high vacuum for at least overnight to remove residual solvent. The thin films were hydrated with 250 mM ammonium sulfate (pH 4.0), sonicated for 10 min, and size-controlled liposomes were prepared using the extruder as described above. Next, the external liposomal phase was replaced with HBS via dialysis (Slide-A-Lyzer 10 kDa MWCO, Pierce Biotechnology, Rockford, IL, USA) for 24 h against 1000 volumes of HBS. The concentration of CHOL was determined using a cholesterol E-Wako kit (Wako Pure Chemical) and a microplate reader (Wallac 4000 ARVO multi-label counter; PerkinElmer, Waltham, MA, USA) in order to estimate the concentrations of the various liposome preparations. Neutral PtCQ-loaded liposomes were prepared by mixing PtCQ solution in HBS (0.65 mg/ml) with the neutral liposomal solution at three drug-to-lipid ratios (1:2.5, 1:5 and 1:7 (w/w) and incubated at 60˚C for 60 min for drug loading. The cationic PtCQ-loaded liposomes were prepared by using a drug/lipid ratio of 1:7 (w/w). The mean size, PDI, and zeta

potential were measured using Zetasizer Nano ZS90 (Malvern) as described above and the EE was calculated as described in "Determination of the EE."

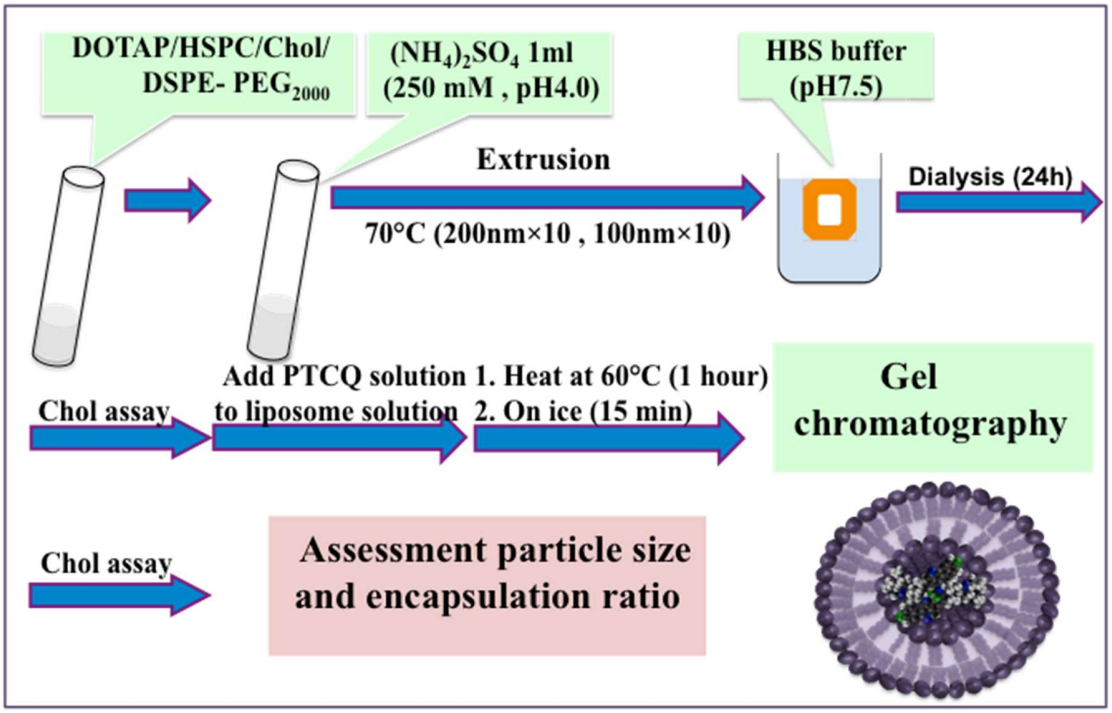

Fig. 9 Preparation of PtCQ-liposomes by thin drug-lipid film

2.2.5 Determination of the EE

For PtCQ-loaded liposomes prepared using the thin drug-lipid film method, the sample was ultracentrifuged (2.1×10^4 g, 4˚C, minimum 30 min) and the pellet was resuspended in HBS buffer. The concentration of the encapsulated drug was measured by absorbance at 343 nm using a UV-visible spectrophotometer (UV-1800, Shimadzu, Kyoto, Japan) after completely disrupting the liposomes using 2% Triton X-100. The absorbance was converted into drug concentration using a standard curve. The EE was calculated using the previously reported equation (Ramana et al., 2010):

EE = (Drug Encapsulated / Total Drug) × 100%

For PtCQ-loaded liposomes prepared using the remote-loading method, the samples were cooled and applied onto a gel filtration column (CL-4B, Sigma Aldrich, Saint Louis, MO, USA) equilibrated with HBS to remove unencapsulated PtCQ. The liposome fraction of the eluate was collected, the concentration of lipid was determined again, and the concentration of the encapsulated drug was measured as described above.

2.2.6. Measurement of drug release from PtCQ-loaded liposomes under storage conditions

All PtCQ-liposomal formulations were stored at 4˚C. As a typical experiment, aliquots (100 µl) were withdrawn at specified time points (0, 1, 2, 4 and 8 weeks),

diluted to 1 ml with HBS buffer, and ultracentrifuged (2.1×10^4 g, 4˚C, 30 min) using Amicon filters (MWCO, 10K; Millipore, Bedford, MA, USA) to separate the released PtCQ. The released PtCQ was measured by absorbance at 343 nm as described above. The percentage of PtCQ released from the liposomes was calculated using the previously reported formula (Aditya et al., 2012):

Drug release (%) = (PtCQ released / Total PtCQ) × 100

Where "PtCQ released" indicates the amount of released PtCQ collected at a specified time point t and "Total PtCQ" indicates the total amount of PtCQ entrapped in the liposomes.

2.2.7 Measurement of drug release from liposomes under *in vitro* culture conditions (release test)

As a typical experiment, 1 ml of liposomal solution was mixed with 1 ml of RPMI 1640 medium (Wako Pure Chemical) supplemented with 10% heat-inactivated fetal bovine serum (Invitrogen, Carlsbad, CA, USA) and the samples were incubated at 37˚C in a humidified incubator in an atmosphere of 5% CO_2/95% air. Aliquots (100 μL) were withdrawn at specified time points (0, 1, 3, 6, 24, 48 and 72 hours), diluted to 1 ml with HBS buffer, and ultra-centrifuged to separate the released PtCQ (2.1×10^4 g, 4˚C, 30 min). The percentage of PtCQ released was determined as in **section 2.6**. The chloroquine absorbance at 343 nm was unaffected by the culture medium, and the standard curve was unaffected, as shown in **Fig. 10.**

2.2.8 Statistical Analysis

All data shown here are represented in "mean value ± standard deviation (S.D.)". An ordinary one-way ANOVA (followed by Tukey's or Dunnett's multiple comparison test), and a two-way ANOVA with (Bonferroni post-test or Dunnett's multiple comparison test) were used to assess statistical significance by using GraphPad Prism (GraphPad Software Inc., CA, USA). $P < 0.05$ was regarded as statistically significant.

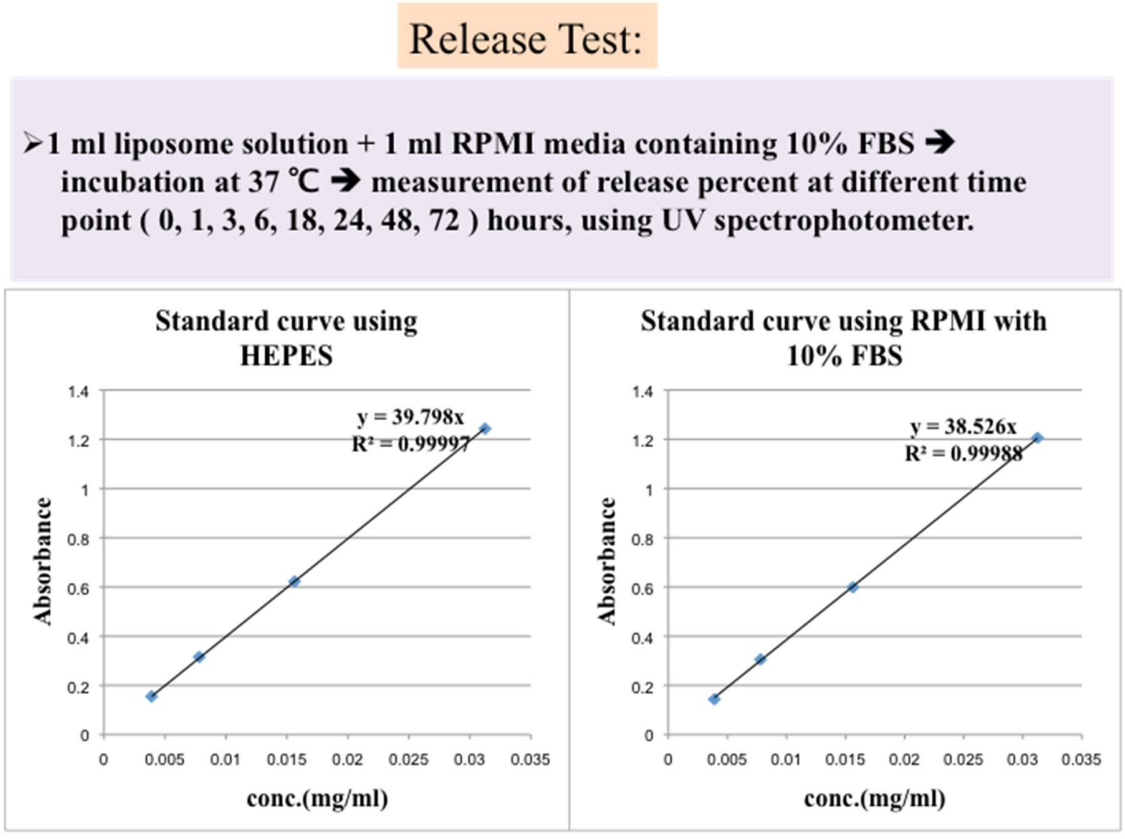

Fig. 10 Standard curve using HEPES and FBS

2.3. Results and discussion

2.3.1 Synthesis and characterization of the Pt(CQDP)2(Cl)2 complex

The platinum-chloroquine diphosphate complex was synthesized and isolated in water at room temperature. A mixture of $K_2[PtCl_4]$ and CQDP was prepared to displace two chloride ligands, leading to the new PtCQ complex that was isolated in good yield as a pink solid precipitate (**Fig. 11)**. The complex was characterized by elemental analysis, and UV-visible, IR and proton-NMR spectroscopy (for analysis data details, see **section 2.2** and **Fig. 12**). The complex is slightly soluble in water and insoluble in organic solvents except DMSO. The elemental analysis of this complex is in agreement with the molecular formula proposed. The IR spectrum of the complex shows peaks clearly associated with the presence of coordinated CQDP. In the ^1H NMR spectrum, the ^1H chemical shift variation of each signal with respect to that of the free ligand reported previously (Navarro et al., 2011) was similar and used to deduce the mode of bonding of CQDP to the metal. The largest shift with respect to the free ligand (CQDP) was observed for NH and H1′ as they are the nearest protons to the N-atom bonded to the metal, indicating that CQDP is bound to platinum through the nitrogen of the secondary amine.

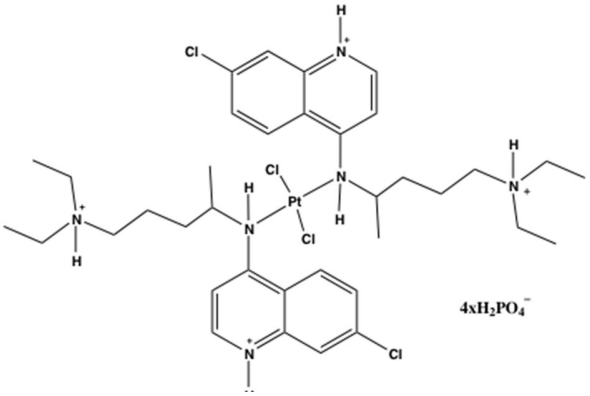

Fig. 11 Chemical structure of platinum chloroquine diphosphate dichloride

Fig. 12 Spectral characterization of the PtCQ complex (A) UV-Vis (B) IR

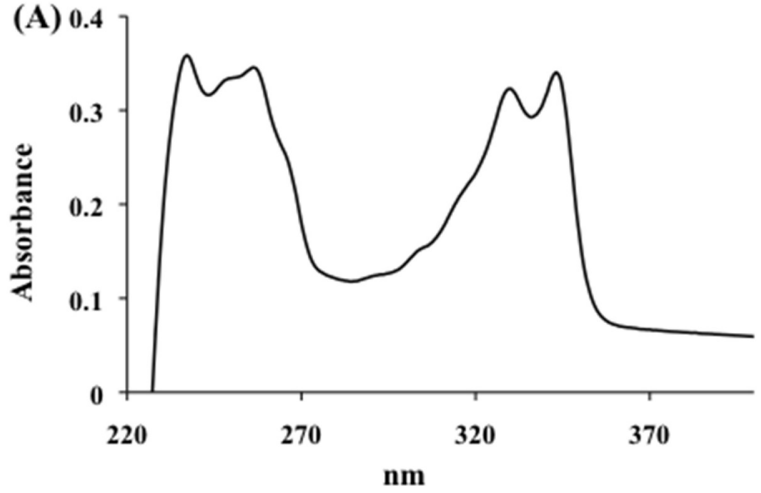

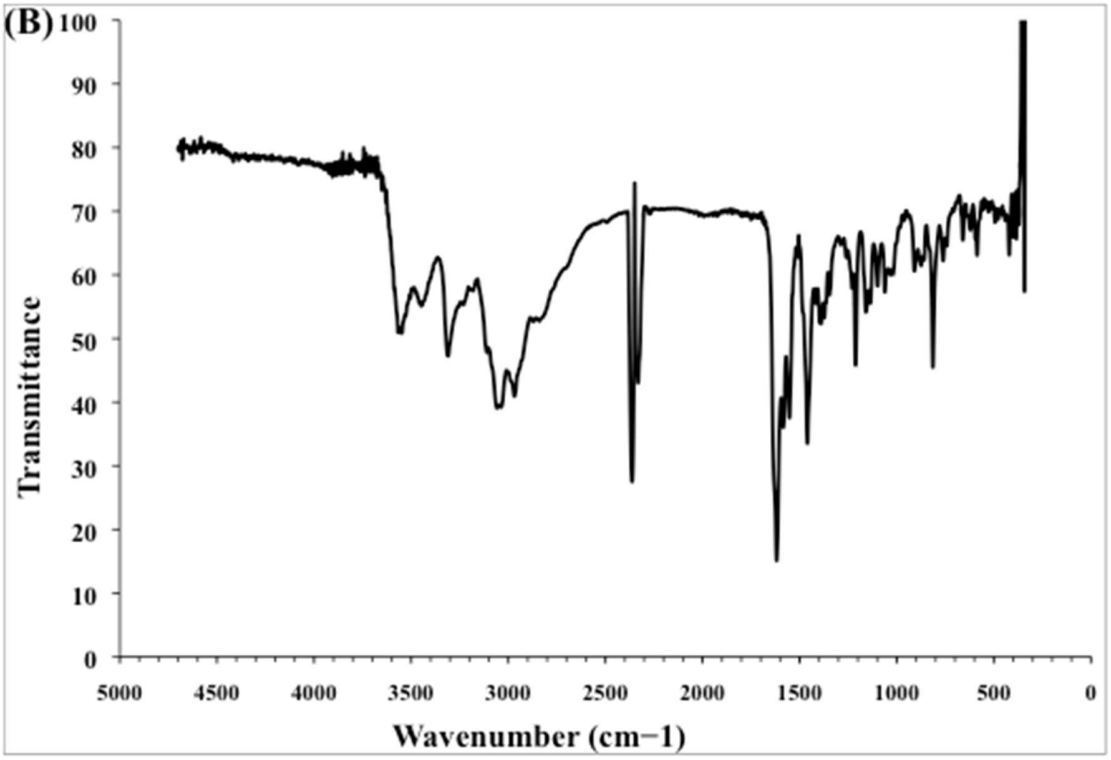

Fig. 12 Spectral characterization of the PtCQ complex (C) proton-NMR

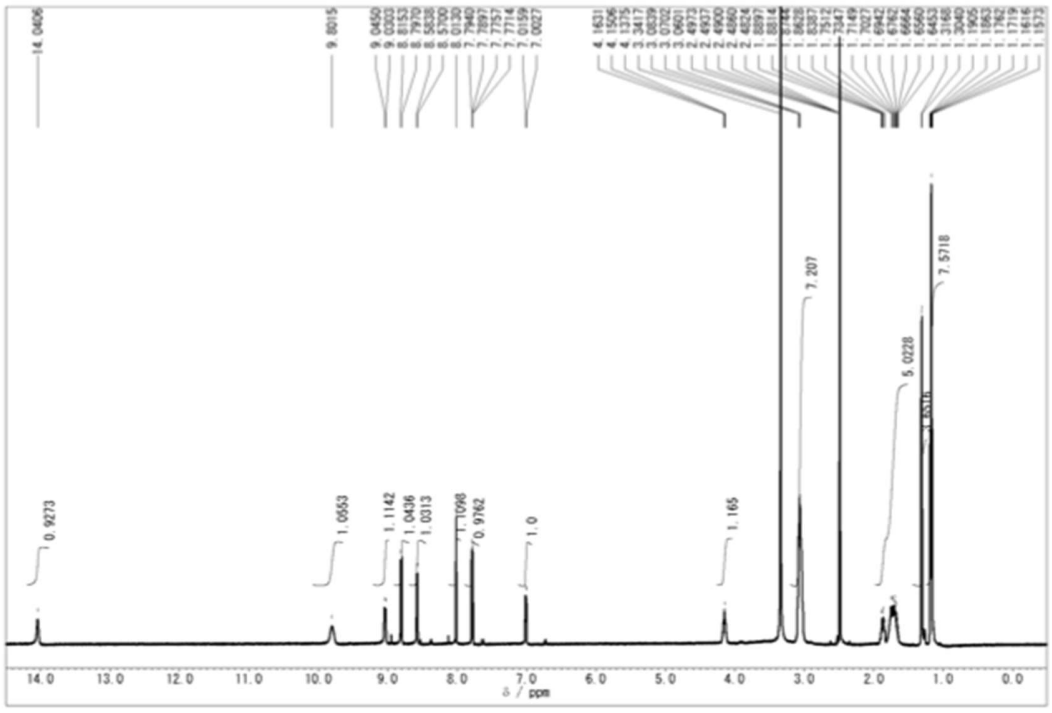

2.3.2. PtCQ-loaded liposomes prepared using the thin drug-lipid film method

The high lipophilicity of metal chloroquine complexes has been previously reported (Navarro et al., 2014) and the preparation of highly stable lipophilic cisplatin complex/liposomes with high encapsulation ratios has been achieved (Khokhar et al., 1991). Consequently, in this study we succeeded in loading the PtCQ complex into neutral and cationic liposomes at reasonable drug-to-lipid ratios by incorporating the drug into the lipid phase using the thin drug-lipid film method. As shown in **Table 1**, the PtCQ-loaded liposomes had uniform sizes ranging from about 105 nm to 143 nm and a narrow size distribution (PDI < 0.097). Furthermore, the zeta potential of PEGylated liposomes was changed from low negative (-7.1 ± 0.5 mV) of the neutral liposomes (1:7) to low positive (10.6 ± 0.9 mV, Cat.20) of the cationic liposomes (1:7). The negative charge of the neutral liposomes is due to the presence of negatively charged phosphate group in DSPE-PEG$_{2000}$ (Woodle et al., 1992). In addition, **Fig. 13** reveals that the cationic lipid content clearly affects the drug loading in the thin drug-lipid film method. Based on the statistical study, the addition of 5 mol% of the cationic lipid DOTAP at low liposome concentration (7 mg) has a significant decrease ($p = 0.0076$) on the EE% of Cat.20 compared to Cat.5, however it has no significant effect ($p > 0.05$) on the EE% of Cat.5 and Cat.20 compared to neutral liposomes. On the other hand, at higher liposome concentration (14 mg), there is a significant decrease ($p < 0.0001$) on the EE% of Cat.20 compared to Cat.5 and the neutral liposomes, however no significant effect ($p > 0.05$) was noticed in the EE% of Cat.5 compared to the neutral liposomes. The decrease in the

EE% with the increase of the cationic lipid content could be due to the electrostatic repulsion between the cationic drug and the cationic lipid such as DOTAP.

Table 1. PtCQ-liposomes loaded by thin drug–lipid film method

Drug : Lipid (w/w) (HSPC/DOTAP/CHOL/ $DSPE\text{-}PEG_{2000}$)	Particle size (nm)	PDI	Zeta potential (mV)
1:7 (55:45:5) (Neut.)	133 ± 11	0.06 ± 0.01	-7.1 ± 0.5
1:7 (50:5:45:5) (Cat.5)	134 ± 11	0.07 ± 0.01	3.6 ± 0.6
1:7 (35:20:45:5) (Cat.20)	121 ± 6	0.04 ± 0.04	10.6 ± 0.9
1:14 (55:45:5) (Neut.)	143 ± 7	0.08 ± 0.02	-6.4 ± 0.8
1:14 (50:5:45:5) (Cat.5)	132 ± 4	0.10 ± 0.01	5.1 ± 0.7
1:14 (35:20:45:5) (Cat.20)	105 ± 4	0.03 ± 0.02	10.0 ± 0.6

Neutral and cationic formulations with drug–lipid (1:7, 1:14 w/w) have been prepared. The neutral lipids have been mixed with the molar ratio (55:45:5). The cationic lipids have been mixed with the molar ratio (5:50:45:5) and (35:20:45:5). Data represent the mean ± S.D. (n = 3).

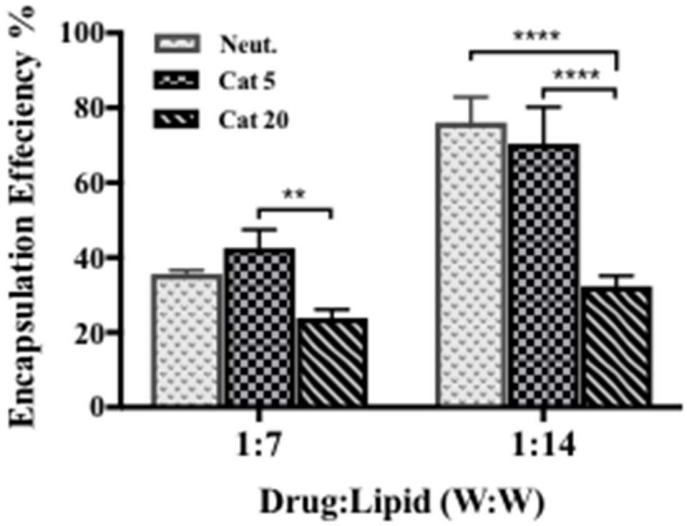

Fig. 13. The EE of liposomes prepared using the thin drug–lipid film method

Three formulations were prepared, at drug to lipid ratios of 1:7, 1:14 (w/w). Data represent the mean ± S.D. (n = 3), (**** $p < 0.0001$, ** $p = 0.0076$). The information about liposomal composition is written in Table 1.

2.3.3 PtCQ-loaded liposomes prepared using the remote-loading method

To our knowledge, this is the first report describing the encapsulation of the PtCQ complex into liposomes using an ammonium sulfate gradient and the results are promising. The rate of loading and the stability of the loaded drug in the intra-liposomal medium mainly depend on the properties of i) the loaded drug, ii) the intra-liposomal medium, and iii) the liposome bilayer, as discussed below.

(i) Properties of the loaded drug:

Chemical compounds can be categorized as hydrophilic compounds, amphiphilic compounds, and hydrophobic compounds. Hydrophilic compounds do not interact with the liposome bilayer and can be encapsulated in the aqueous phase of the liposome interior. Hydrophobic compounds integrate into the liposome bilayer. Amphiphilic compounds may be amenable to high loading due to their possible high affinity for the liposomal membrane or may be remotely loaded into the intra-liposomal aqueous phase by using a pH gradient. CQ is a diprotic amphiphilic weak base with two proton-binding groups: the side chain terminal amine (pKa_1 = 10.2) and the quinoline nitrogen atom (pKa_2 = 8.4). Accordingly, unprotonated CQ can be driven by a pH gradient across a parasite's food vacuole membrane and thus accumulate in the acidic food vacuole.

CQ can be actively encapsulated by applying a pH gradient (Qiu et al., 2008; Madden et al., 1990), during which it is protonated to the diproton form following exposure to the intra-liposomal acidic medium, then captured inside the liposomes due to the low permeability of the liposomal bilayer membrane to the protonated drug (Qiu et al., 2008). In the present study we used the ammonium sulfate gradient to load PtCQ into

liposomes composed mainly of neutral or cationic saturated phospholipids with an EE of almost 100%, as shown in **Figure 14** and **Figure 15**.

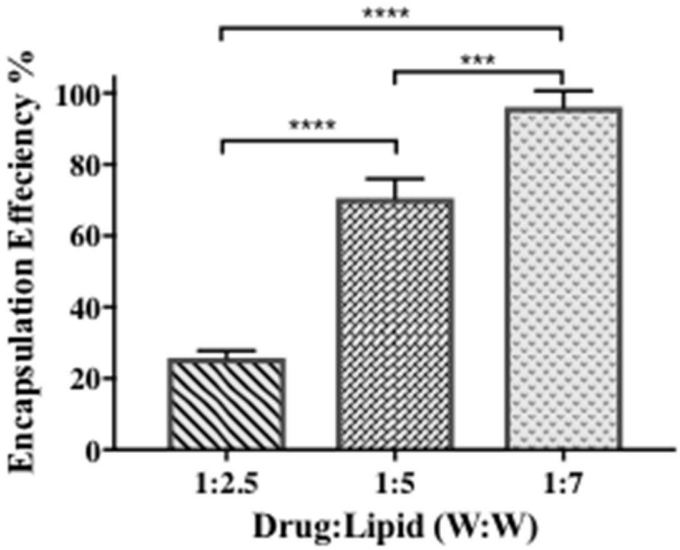

Fig. 14. Effect of increasing the liposomal content on the EE of PtCQ loaded inside neutral liposomes prepared using the remote loading method

Three formulations were prepared, at drug to lipid ratios of 1:2.5, 1:5 and 1:7 (w/w). Data represent the mean ± S.D. (n = 3). Statistical data infers that each group is significantly different (****p < 0.0001, ***p = 0.0008). The information about liposomal composition is written in Table 2.

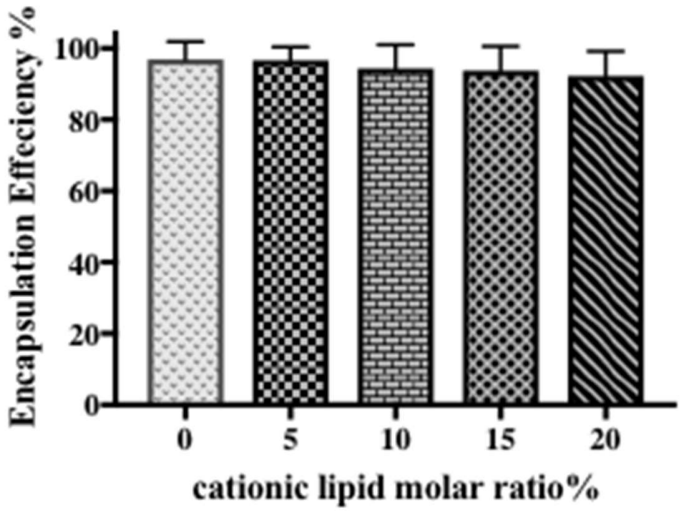

Fig. 15. Effect of increasing the cationic lipid content (DOTAP) on the EE of PtCQ loaded inside cationic liposomes prepared using the remote loading method

Five formulations were prepared (0, 5, 10, 15, 20 mol% as cationic lipid). The drug-to-lipid ratio is 1:7 (w/w). Data represent the mean ± S.D. (n = 4). The information about liposomal composition is written in Table 3.

(ii) Intra-liposomal medium properties:

Various chemical gradients have been used to create a trans-membrane potential as a driving force to facilitate the loading of a drug through an active loading mechanism. For example, ammonium sulfate induces a potential gradient for weak bases and acids and this gradient remains stable for over six months for liposomal formulations stored below the transition temperature of the phospholipids (Haran et al., 1993). Furthermore, lipophilic amino-containing drugs can be partitioned into the lipid bilayer, resulting in a drug gradient through the lipid bilayer that aids the influx of the drug from the outside to the inside (Harrigan et al., 1993).

In the present study, we loaded the PtCQ complex into neutral liposomes using a pH gradient and the trans-membrane potential generated by an ammonium sulfate gradient as driving forces. Following hydration of the PtCQ-loaded liposomes using an ammonium sulfate solution, an equal concentration of ammonium sulfate is found outside and inside the liposomes. Removal of the outside ammonium sulfate solution by dialysis leads to an ammonium sulfate gradient in which the concentration of ammonium sulfate inside the liposomes is greater than that outside and the gradient is due to the large difference in the permeability coefficient through lipid bilayer as mentioned before (Haran et al., 1993). The higher concentration of ammonium inside the liposome causes the efflux of neutral ammonium, leaving the protons inside the liposome. This ammonium gradient results in the influx of the PtCQ into the acidic intra-liposomal medium and thus its encapsulation. The drug may be tetra-protonated due to the presence of two chloroquine molecules in the complex. The outside-inside pH gradient was 7.5–4

to give a pH gradient equal to 3.5 units (ΔpH = (external pH − internal pH) = 3.5) since this produces a much higher inside concentration of the weak base compared to the outside concentration. As shown in **Fig. 14** and **Table 2,** PtCQ-loaded liposomes were prepared with different drug-to-lipid weight ratios and the maximum EE was obtained at a drug-to-lipid ratio of 1:7 (w/w). In a preliminary experiment, the loading of PtCQ was compared using ammonium sulfate or citrate buffer and the EE was found to be higher with ammonium sulfate, perhaps due to the high permeability coefficient of the NH_3 molecule, which causes fast diffusion of neutral ammonia to the external medium of the liposomes. Each diffusing NH_3 molecule leaves one proton inside the liposome, thus acidifying the intra-liposomal medium and resulting in a pH gradient and influx of the drug (Haran et al., 1993). The pH gradient had a greater effect on CQ, which has two amino moieties, than on a weak base with one amino moiety (Qiu et al., 2008).

(iii) Liposome bilayer properties

It was previously demonstrated that drug-loaded liposomes prepared by the remote loading method and comprising saturated lipids can be maintained at 4˚C for at least six months without deterioration (Haran et al., 1993). Liposomes composed of saturated lipids can maintain a pH gradient due to the relatively high transition temperature of the bilayer. In the present work, we used the saturated lipid HSPC to construct the membrane of PtCQ-loaded liposomes generated using the remote loading method. The demonstrated stability of the PtCQ-loaded liposomes under storage and culture conditions verifies the ability of this saturated lipid bilayer to maintain a specified pH gradient and retain the drug in the interior phase of the liposome as long as the

temperature does not exceed the transition temperature of the lipid, thus preventing thermal mobility that could disrupt the membrane required for maintaining the pH gradient (Qiu et al., 2008). We studied the effect of temperature on drug loading at two temperatures below the transition temperature 60˚C, after incubation for one hour and obtained maximum loading at 60˚C as described below.

Table 2. PtCQ-liposomes loaded by ammonium sulfate gradient

Drug : Lipid (w/w) Neutral liposomes	Particle size (nm)	Polydispersity index	Zeta potential (mV)
1:2.5	109 ± 3	0.05 ± 0.01	-7.2 ± 1.8
1:5	109 ± 3	0.06 ± 0.02	-7.8 ± 1.2
1:7	108 ± 1	0.04 ± 0.01	-7.9 ± 1.0

The neutral lipids have been mixed with the molar ratio (HSPC/CHOL/DSPE-PEG_{2000} = 55:45:5). Three different formulations with drug–lipid (1:2.5, 1:5, 1:7 w/w) have been prepared. Data represent the mean ± S.D. (n = 3).

2.3.4 Cationic PtCQ-loaded liposomes produced using the remote-loading method

Five types of cationic PtCQ-loaded liposomes with a drug-to-lipid ratio of 1:7 (w/w) but differing in the ratios of the constituent lipids were prepared and characterized, and the results are shown in **Table 3**. The PtCQ-loaded cationic liposomes has uniform sizes about 130 nm and a narrow size distribution (PDI < 0.05). It was reported that the cationic liposomes demonstrate an enhanced cellular uptake compared to the neutral liposomes, it could be due to the electrostatic interaction between the positive charge and the cell (Zhao et al., 2011). Additionally, the increase of cationic lipids in liposomes could lead to a higher affinity for the anionic sites, however it could result in their aggregation in the bloodstream through electrostatic interactions with the anionic species in the blood and thus increase their uptake by the RES (reticuloendothelial system) (Zhao et al., 2011). Liposomes are typically modified with PEG (PEGylation) to form a water layer that could prevent protein adsorption onto the liposome surface and decrease the uptake of PEG-liposomes by macrophages and thus help in prolonging the lifetime of liposomes in the blood circulation (Kraft et al., 2014). The partial coating of cationic particles with PEG masks the values of zeta potential (electric potential across a double membrane surface), however it can't prevent them from binding to the cells and the biodistribution completely. Moribe et al., reported that the inclusion of 0 to 10% PEG sharply decreases zeta potential of the liposome (Moribe et al., 1997). For this reason typically 5–10 mol% of PEG is enough to delay the recognition of liposomes by immune system cells. This concentration could retain a significant cationic charge and binding to

the cells. Consequently, All formulations prepared in this study were PEGylated with 5 mol %. Additionally, it has been reported that the adhesion of the liposome membrane to the cell depends on the ratio of the liposome–cell charge, thus the probability of adhesion is maximized at a finite polymer layer thickness in case of the cationic liposomes are overcharged compared to the cell (Dan et al., 2002). Accordingly, in this study, several PtCQ-loaded liposomes with different molar ratio of the cationic lipid (DOTAP, 0, 5, 10, 15 and 20 mol%) were prepared to provide stable cationic PtCQ-loaded liposomes that could selectively bind to erythrocytes. **Table 3** reveals that the zeta potential of PEGylated cationic liposomes changes from low negative (-7.5 ± 1.3) for (Cat.0) to neutral (-0.4 ± 0.7, Cat.10), and to low positive (10.7 ± 3.0, Cat.20).

The addition of negatively charged lipids to liposomes generated using the passive loading method can increases EE due to electrostatic interaction between the positively charged chloroquine and the negatively charged liposomes. However, characterization of the PtCQ-loaded liposomes prepared using the thin drug-lipid film method presented in **section 3.2** confirmed that the EE of cationic liposomes decrease with increasing the cationic lipid content and this could be due to the electrostatic repulsion between the cationic drug and the cationic lipid. In contrast, **Fig. 15** reveals that the different cationic PtCQ-loaded liposomes prepared by ammonium sulfate gradient (Cat.5, Cat.10, Cat.15, and Cat.20) have no significant effect ($p > 0.6559$) on EE% compared to Cat.0 (96.9 ± 5.0%). This result confirms that the most of PtCQ loaded by

ammonium sulfate gradient is not bilayer-associated, in good agreement with a previous report (Haran et al., 1993).

Table 3. PtCQ-liposomes loaded by ammonium sulfate gradient

Drug : Lipid (w/w) Cationic liposomes HSPC/DOTAP/ CHOL/DSPE-PEG$_{2000}$	Particle size (nm)	PdI	Zeta potential (mV)
55:0:45:5 (Cat.0)	128 ± 7	0.03 ± 0.02	-7.5 ± 1
50:5:45:5 (Cat.5)	112 ± 4	0.05 ± 0.01	-3.3 ± 1
45:10:45:5 (Cat.10)	129 ± 5	0.04 ± 0.02	-0.4 ± 1
40:15:45:5 (Cat.15)	115 ± 2	0.05 ± 0.03	8.1 ± 1
35:20:45:5 (Cat.20)	114 ± 4	0.05 ± 0.01	10.7 ± 3

The cationic lipids have been mixed with different molar ratios. Five different formulations with HSPC–DOTAP (55:0, 50:5, 45:10, 40:15, 35:20) have been prepared. Data represent the mean ± S.D. (n = 3, 4).

2.3.5 Drug release from cationic PtCQ-loaded liposomes under storage conditions (storage test)

The stability of cationic PtCQ-loaded liposomes (cat.0, cat.5, cat.10, cat.15, cat.20) loaded using the ammonium sulfate gradient (drug-to-lipid ratio 1:7 (w/w)) was studied during eight weeks' storage at 4˚C. **Fig. 16** reveals that there is no significant release ($p > 0.05$) of the drug at different cationic PtCQ-loaded liposomes after eight weeks' storage at 4˚C, compared to Cat.0 (5.7 ± 4.9 %). This demonstrates the utility of the ammonium sulfate gradient method for incorporating amphiphilic drugs into stable liposomes containing a saturated lipid (HSPC). It was reported that the addition of PEG stabilizes liposomes due to repulsive barrier resulted from steric pressure forces and charged phosphate moieties (Woodle et al., 1992; Needham et al., 1992). Additionally, the presence of CHOL stabilizes liposomal formulations, as reported previously (Briuglia et al., 2015; Lee et al., 2005).

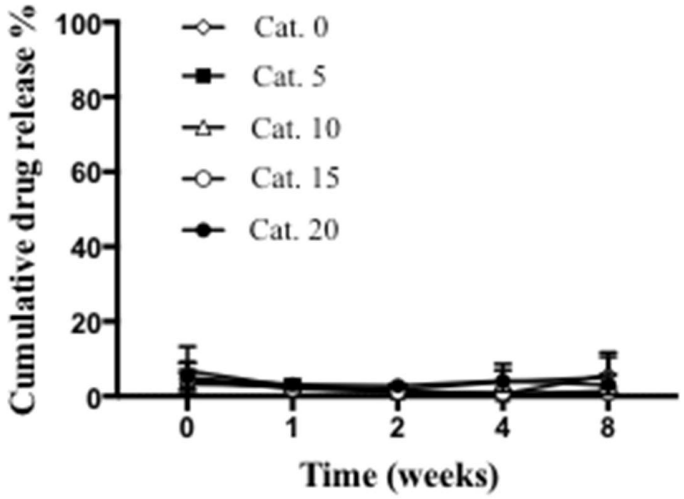

Fig. 16. Release pattern of PtCQ from cationic liposomes, Prepared by Remote Loading Method, in HEPES Buffer during Storage at 4°C. PtCQ was loaded into the liposomes at a drug-to-lipid ratio of 1:7 (w/w). Data represent the mean ± S.D. (n = 3). Cat. 0, Cat. 5, Cat. 10, Cat. 15 and Cat. 20 are the five formulations of cationic PtCQ-loaded liposomes prepared using different molar ratio of the cationic lipid (DOTAP, 0, 5, 10, 15 and 20 mol %, respectively)

2.3.6 Drug release from cationic PtCQ-loaded liposomes under culture conditions (release test)

A drug release study was carried out using medium containing FBS to mimic *in vivo* conditions. **Figure 17** reveals that the PtCQ liposomes loaded by thin drug-lipid film method (drug to lipid ratio 1:7 (w/w)) have initial burst release equal to 8.9 ± 0.5% of neutral liposomes and equal to 13.2 ± 2.1% of cationic liposomes (Cat.5) at 0 hour. The cause for initial burst release may be due to the adsorption of some drug molecules on the liposome surface during formation of the thin film. Furthermore, after 72 hours, there is a significant drug release ($p = 0.0001$) of Cat.5 compared to neutral liposomes'cumulative release equal to 17.8 ± 2.6%. The cationic liposomes showed a maximum release which is slightly higher than that of neutral liposomes and this could be due to electrostatic repulsion between the cationic drug and the cationic lipid.

The five formulations of cationic PtCQ-loaded liposomes (cat.0, cat.5, cat.10, cat.15, cat.20) loaded using an ammonium sulfate gradient (drug to lipid ratio 1:7 (w/w) described above didn't show initial burst release and showed no significant release ($p > 0.05$) of the drug after 72 hours compared to Cat.0 (4.0 ± 2.3%), as shown in **Figure 18**. This demonstrates that the ammonium sulfate gradient is a promising method for the encapsulation of amphiphilic drugs into liposomes containing a saturated lipid (HSPC). Furthermore, the amount of drug released was sustainably released indicating that liposomes loaded with amphipathic weak bases using an ammonium sulfate gradient can provide controlled release of the loaded molecule. Increasing the cationic lipid from 0% to 20% mole percent has no significant effect on the release of the drug; showing that the

surface charge has no effect on the release of amphipathic weak bases loaded using ammonium sulfate and pH gradients. The slow drug release observed in case of ammonium sulfate gradient loaded PtCQ-liposomes is necessary for long storage and to avoid drug leaking before reaching their target (Moles et al., 2015). Afterward the liposomes would be adsorbed on the cell surface followed by a depletion of the liposomal proton gradient due to the body temperature or liposomes-cell interaction episodes. This depletion leads to accumulation of the weak basic drugs inside the RBC due to the electrochemical gradient resulted from the phospholipid asymmetry in RBC membranes, which maintains negatively charged membranes.

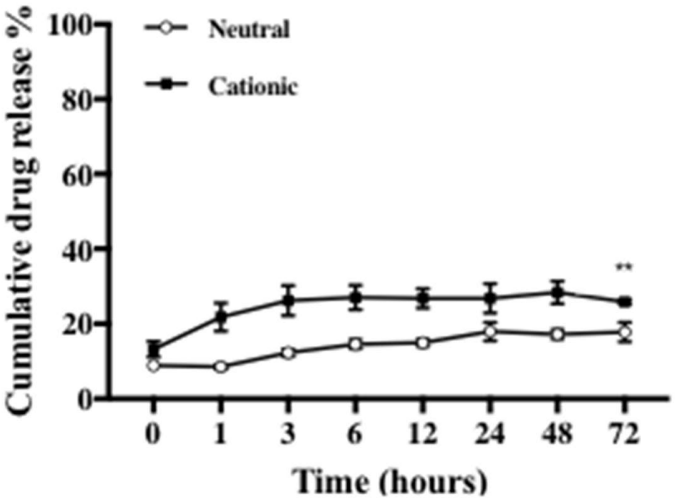

Fig. 17. Release pattern of PtCQ from neutral and cationic liposomes, Prepared by thin drug–lipid film method, under culture conditions. PtCQ-loaded liposomes were incubated in medium containing 10 % FBS at 37°C. PtCQ was loaded into the liposomes at a drug-to-lipid ratio of 1:7 (w/w). Data represent the mean ± S.D. (n = 3). (**** $p < 0.0001$, *** $p = 0.0007$, ** $p = 0.0024$) compared to neutral liposomes.

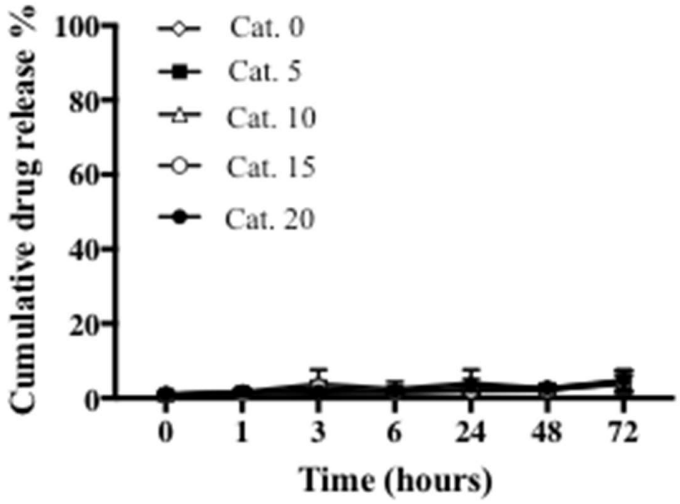

Fig. 18. Release pattern of PtCQ from cationic liposomes, Prepared by PtCQ-loaded liposomes were incubated in medium containing 10 % FBS at 37°C. PtCQ was loaded into the liposomes at a drug-to-lipid ratio of 1:7 (w/w). Data represent the mean ± S.D. (n = 3). Cat. 0, Cat. 5, Cat. 10, Cat. 15 and Cat. 20 are the five formulations of cationic PtCQ-loaded liposomes prepared using different molar ratio of the cationic lipid (DOTAP, 0, 5, 10, 15 and 20 mol %, respectively)

2.4. Conclusion

This chapter described the synthesis and characterization of the trans-platinum-chloroquine complex (PtCQ) and the application of two methods to generate PtCQ-loaded liposomes: the thin drug-lipid film and the remote loading methods. Liposomes of uniform diameter were prepared using the thin film hydration and extrusion technique and the PtCQ was encapsulated in the liposomes. The most efficient encapsulation was obtained at a drug-to-lipid ratio of 1:7 (w/w) using the ammonium sulfate gradient active loading method. This approach provided liposomal formulations capable of sustaining a proton gradient for the weak basic drug PtCQ and the encapsulation efficiency was approximately 100%. High intra-liposomal retention levels of 93% the drug inside different cationic liposomes for several hours under culture and storage conditions were maintained, suggesting that such liposomes hold promise for the future treatment of malaria by targeting *Plasmodium falciparum*. We will study the *in vitro* and *in vivo* effects of cationic PtCQ-loaded liposomes on this parasite and the encapsulation of other metal-CQ complexes in the future.

2.5. References

Abu Lila, A.S., Kizuki, S., Doi, Y., Suzuki, T., Ishida, T., Kiwada, H., 2009. Oxaliplatin encapsulated in PEG-coated cationic liposomes induces significant tumor growth suppression via a dual-targeting approach in a murine solid tumor model. J. Control Release. 137: 8–14.

Aditya, N.P., Chimote, G., Gunalan, K., Banerjee, R., Patankar, S., Madhusudhan, B., 2012. Curcuminoids-loaded liposomes in combination with arteether protects against *Plasmodium berghei* infection in mice. Exp. Parasitol. 131, 292–299.

Baruah, U.K, Gowthamarajan, K., Vanka, R., 2017. Malaria treatment using novel nano-based drug delivery systems. J. Drug Target. 25,567–581.

Briuglia, M-L., Rotella, C., McFarlane, A., Lamprou, D. A., 2015. Influence of cholesterol on liposome stability and on in vitro drug release. Drug Delivery Translat. Res. 5, 231–242.

Campbell, R.B, Ying, B., Kuesters, G.M., Hemphill, R. 2009. Fighting cancer: from the bench to bedside using second-generation cationic liposomal therapeutics. J. Pharm. Sci. 98, 411–429.

Campbell, R.B., Fukumura, D., Brown, E.B., Mazzola, L.M., Izumi, Y., Jain, R.K., Torchilin, V.P., and Munn, L.L., 2002. Cationic charge determines the distribution of liposomes between the vascular and extravascular compartments of tumors. Cancer Res. 62, 6831–6836.

Dan, N., 2002. Effect of liposome charge and PEG polymer layer thickness on cell-liposome electrostatic interactions. Biochim. Biophys. Acta. 1564, 343–348.

Föller, M., Bobbala, D., Koka, S., Huber, S. M., Gulbins, E. and Lang, F., 2009. Suicide for survival–death of infected erythrocytes as a host mechanism to survive malaria. Cell Physiol. Biochem. 24, 133–140.

Greenwood, B.M., Fidock, D.A., Kyle, D.E., Kappe, S.H., Alonso, P.L., Collins, P.L.F.H., Duffy, P.E, 2008. Malaria: progress, perils, and prospects for eradication. J Clin Invest. 118, 1266–1276.

Haran, G., Cohen, R., Bar, L.K. and Barenholz, Y., 1993. Transmembrane ammonium sulfate gradients in liposomes produce efficient and stable entrapment of amphipathic weak bases. Biochim. Biophys. Acta 1151, 201–215.

Harrigan, P.R., Wong, K.F., Redelmeier, T.E., Wheeler, J.J. and Cullis, P.R., 1993. Accumulation of doxorubicin and other lipophilic amines into large unilamellar vesicles in response to transmembrane pH gradients. Biochim. Biophys. Acta. 1149, 329–338.

Isacchi1, B., Arrigucci, S., la Marca, G., Camilla Bergonzi, M., Vannucchi, M.G., Novelli, A., and Bilia, A.R., 2011. Conventional and long-circulating liposomes of artemisinin: preparation, characterization, and pharmacokinetic profile in mice. J. of Liposome Res. 21, 237–244.

Johnstone, S.A., Masin, D., Mayer, L., Bally, M.B., 2001.Surface-associated serum proteins inhibit the uptake of phosphatidylserine and poly (ethylene glycol) liposomes by mouse macrophages. Biochim. Biophys. Acta. 1513, 25–37.

Khokhar, A. R., Al-Baker, S., Brown, T. and Perez-Soler, R., 1991. Chemical and biological studies on a series of lipid-soluble (trans-(R,R)- and -(S,S)-1,2-diaminocyclohexane) platinum(II) complexes incorporated in liposomes. J. Med. Chem. 34, 325–329.

Kraft, J. C., Freeling, J. P., Wang, Z. and Ho, R. J. Y., 2014. Emerging research and clinical development trends of liposome and lipid nanoparticle drug delivery systems. J. Pharm. Sci. 103, 29–52.

Laouini, A., Jaafar-Maalej, C., Limayem-Blouza, I., Sfar, S., Charcosset, C. and Fessi, H., 2012. Preparation, Characterization and Applications of Liposomes: State of the Art. J. Colloid Sci. and Biotech. 1, 147–168.

Lee, S-C, Lee, K-E, Kim, J-J and Lim, S-H, 2005. The effect of cholesterol in the liposome bilayer on the stabilization of incorporated retinol. J. Liposome Res. 15, 157–166.

Levchenko, T.S, Rammohan, R., Lukyanov, A.N, Whiteman, K.R, Torchilin, V.P, 2002. Liposome clearance in mice: the effect of a separate and combined presence of surface charge and polymer coating. Int. J. Pharm. 240, 95–102.

Li, L.H., Hui, S.W., 1997. The effect of lipid molecular packing stress on cationic liposome-induced rabbit erythrocyte fusion. Biochim. Biophys. Acta. 1323, 105–16.

Madden, T.D., Harrigan, P.R., Tai, L.C.L., Bally, M.B., Mayer, L.D., Redelmeier, T.E., Loughrey, H.C, Tilcock, C.P, Reinish, L.W, Cullis, P.R., 1990. The accumulation of drugs within large unilamellar vesicles exhibiting a proton gradient: a survey. Chem. Phys. Lipids. 53, 37–46.

Miller, L.H., Ackermen, H.C., Su, X-Z, Wellems, T.E., 2013. Malaria biology and disease pathogenesis: insights for new treatments. Nat. Med. 19, 156–167.

Moles, E., Urbán, P., Jiménez-Díaz, M.B., Viera-Morilla, S., Angulo-Barturen, I., Busquets, M. A., Fernàndez-Busquets, X., 2015. Immunoliposome-mediated drug delivery to Plasmodium-infected and non-infected red blood cells as a dual therapeutic/prophylactic antimalarial strategy. J. Control Release. 210, 217–229.

Moribe, K., Maruyama, K, Iwatauru, M., 1997. Estimation of surface state of Poly(ethylene glycol)-coated liposomes using an aqueous two-phase partitioning technique. Chem. Pharm. Bull. 45, 1683–1687.

Navarro, M., Castroa, W., Higuera-Padillaa, A.R, Sierraaltab, A., Abadc, M.J., Taylorc, P., and Roberto, A., 2011.Sánchez-Delgadod, Synthesis, characterization and biological activity of trans- platinum (II) complexes with chloroquine. J. Inorg. Biochem. 105, 1684–1691.

Navarro, M., Castro, W., Madamet, M., Amalvict, R., Benoit, N., Pradines, B., 2014. Metal-chloroquine derivatives as possible anti-malarial drugs: evaluation of anti-malarial activity and mode of action. Malar. J. 13, 471.

Needham, D., Mclntosh, T.J. and Lasic, D.D., 1992. Repulsive interactions and mechanical stability of polymer-grafted lipid membranes. Biochim. Biophys. Acta. 1108, 40–48.

Obata, Y., Tajima, S., Takeoka, S., 2010. Evaluation of pH-responsive liposomes containing amino acid- based zwitterionic lipids for improving intracellular drug delivery in vitro and *in vivo*. J. Control Release.142, 267–276.

Peeters, P.A.M., Huiskamp, C.W.E.M., Eling, W.M.C. and Crommelin, D.J.A., 1989. Chloroquine containing liposomes in the chemotherapy of murine malaria. Cambridge J., Parasitol. 98, 381–386.

Qiu, L., Jing, N., Jin, Y., 2008. Preparation and *in vitro* evaluation of liposomal chloroquine diphosphate loaded by a transmembrane pH-gradient method. Int. J. Pharm. 361, 56–63.

Ramana, L.N., Sethuraman, S., Ranga U., and Krishnan, U.M., 2010. Development of a liposomal nanodelivery system for nevirapine. J. Biomed. Sci. 17, 57.

Santos-Magalhães, N. S., Mosqueira, V. C. F., 2010. Nanotechnology applied to the treatment of malaria. Adv. Drug Deliv. Rev. 62, 560–575.

Stebelska, K., Wyrozumska, P., Sikorski, A.F., 2006. PS exposure increases the susceptibility of cells to fusion with DOTAP liposomes. Chem. Biol. Interact. 160, 165–174.

Tagami, T., Yanai, H., Terada, Y. and Ozeki, T. 2015. Evaluation of Phosphatidylserine-Specific Peptide-Conjugated Liposomes Using a Model System of Malaria-Infected Erythrocytes. Biol. Pharm. Bull. 38, 1649–1651.

Tagami, T., Kubota M., and Ozeki, T., 2015. Effective remote loading of doxorubicin into DPPC/Poloxamer 188 hybrid liposome to retain thermosensitive property and the assessment of carrier-based acute cytotoxicity for pulmonary administration. J. Pharm. Sci. 104, 3824–3832.

Tagami, T., Ernsting, M.J., Li, S-D, 2011. Efficient tumor regression by a single and low dose treatment with a novel and enhanced formulation of thermosensitive liposomal doxorubicin. J. Control Release. 152, 303–309.

Urbán, P., Estelrich, J., Cortés, A., Fernàndez-Busquets, X., 2011. A nanovector with complete discrimination for targeted delivery to *Plasmodium falciparum*-infected versus non-infected red blood cells *in vitro*. J. Control Release 151, 202–211.

WHO: World Malaria Report. World Health Organization. (2015).

Woodle, M.C., Collins, L.R., Sponsler, E., Kossovsky, N., Papahadjopoulos, D., Martin, F.J., 1992. Sterically stabilized liposomes reduction in electrophoretic mobility but not electrostatic surface potential. Biophys. J. 61, 902–910.

Woodle, M.C, Lasic, D.L., 1992. Sterically stabilized liposomes. Biochim. Biophys. Acta. 1113, 171–199.

Zhao, W., Zhuang, S., Qi, X-R, 2011. Comparative study of the *in vitro* and *in vivo* characteristics of cationic and neutral liposomes. Int. J. Nanomed. 6, 3087–3098

CHAPTER 3

Curcumin marinosomes as promising nano-drug delivery system for cancer

3.1. Introduction

Lung cancer is the major cause of cancer-related deaths worldwide with the non-small cell lung cancer (NSCLC) accounts about 80 % of all lung cancer cases. Surgical removal is the standard treatment for early-stage NSCLC with the danger of postoperative complications (National Comprehensive Cancer Network Guideline 2018). Platinum-based chemotherapy and radiation are the standard therapies for advanced NSCLC (Mehta et al., 2014). Radiation and chemotherapy may result in a lot of negative side effects, including renal and neurologic toxic effects, aplasia, pneumonitis and pericarditis. In order to augment tumor control and diminish chemotherapy side effects, potential alternatives and non-toxic therapies for lung cancer have to be continuing investigated.

Curcumin, which is a polyphenolic hydrophobic natural compound derived from the rhizomes of *Curcuma longa*, has been used to treat various disorders due to its safety and cost-effectiveness. Curcumin has been reported to target several molecules involved in the multistep carcinogenesis (Mehta et al., 2014). Meaning that curcumin can target tumor suppressor genes, cyclooxygenases and lipoxygenases to induce anti-carcinogenic and anti-inflammatory effects (Hong et al., 2004). Curcumin also suppresses the expression of tumor necrosis factor alpha that is an inflammatory

cytokine to control the progress of most tumor cells. Additionally, curcumin modulates the expression of transcription factors to act as anti-proliferative, anti-inflammatory, anti-angiogenic and anti-metastatic agent (Balasubramanyam et al., 2004; Bharti et al., 2003; Bierhaus et al., 1997; Pendurthi and Rao, 2000; Shishodia et al., 2003). Together these studies implicate that curcumin could be a promising chemopreventive agent for lung cancer treatment. Despite the promising effects of curcumin against cancer and numerous diseases, its light sensitivity, poor solubility in aqueous medium and poor bioavailability are issues make it less useful as a therapeutic agent and have to be overcome in order to avail the entire benefits of this plant-extracted compound (Anand et al., 2007). Nano-formulations of curcumin using liposomes (Li et al., 2005), polymeric nanoparticles (Bisht et al., 2007), lipid nanoparticles (Sou et al., 2008), nanoemulsions (Ahmed et al., 2012), and cyclodextrins (Desai, 2010) have been extensively investigating in order to enhance drug solubility, bioavailability, the therapeutic efficacy and cause controlled release of the drug. Although promising were these attempts, they showed some disadvantages like excipients' high cost, innate cytotoxicity or limited drug loading and entrapment efficiency. Consequently, the encapsulation of curcumin into naturally occurring compound could help to develop a potential anticancer therapy from low-cost and readily available nutaceuticals.

Marinosomes are marine lipid-based liposomes containing a high ratio of polyunsaturated fatty acids (PUFAs) (Moussaoui et al., 2002). Marine PUFAs are divided into two subgroups: omega-6 (n-6) and omega-3 (n-3) that are metabolized and stored in cell membrane phospholipids (Schmitz and Ecker, 2008). They

influence membrane fluidity, regulate a wide range of functions in the body and correct development and functioning of the brain and nervous systems (Das, 2006). In marine lipids, extracted from marine organisms like krill, a large portion of n-3 PUFAs are bound to phospholipids and includes a higher content of n-3 long chain PUFAs such as eicosapentaenoic acid (EPA; 20:5 n-3) and docosahexaenoic acid (DHA; 22:6 n-3) (Peng et al., 2003; Winther et al., 2011). Marine phospholipids have high bioavailability compared with triglyceride are efficiently taken up into body tissues (Wijendran et al., 2002). It is previously reported that a diet including high n-3 long chain PUFA, such as the Japanese and Mediterranean diets, has lower occurrence of cancer (Gerber, 2012). N-3 PUFAs have been used in the prevention and treatment of cancer through various mechanisms (Vaughan et al., 2013). A likely mechanism of cancer prevention through the anti-inflammatory properties of n-3 PUFAs has been reported (Alaarg et al., 2016). Other studies have reported different mechanisms of cancer prevention by n-3 PUFAs including apoptosis, inhibition of angiogenesis, inhibition of metastasis and others (Blanckaert et al., 2010; Iigo et al., 1997; Yin et al., 2017). Actually, n-3 PUFAs are not only beneficial in cancer treatment but also in other diseases that share the same common physiopathological features like unbalanced oxidative stress, inflammation and abnormal cell proliferation (Calder, 2012; Ross et al., 2001).

Despite the promising effects of n-3 PUFAs against cancer and other numerous diseases, it has been reported that their effects are typically observed after long-term oral consumption at a relatively high amount (Geusens et al., 1994; Schmidt et al., 1992). The use of nanomedicine to increase the levels of n-3 PUFAs in

inflamed tissues has been studied (Alaarg et al., 2016). Additionally, effective and low-cost anticancer combination drugs were developed from curcumin with other naturally occurring nutraceuticals (Choudhury et al., 2013). To benefit wholly from the effects of both n-3 PUFAs and curcumin, together nanomedicine with drug combination strategy will be used to propose a novel liposomal formulation of curcumin-loaded PUFAs liposomes (curcumin marinosomes; CURMs, **Fig. 19**). Such liposomal formulation could improve the bioavailability of curcumin, causes controlled release and leads to increased stability, antioxidant and anticancer activity. In this study, the physicochemical characteristics of CURMs and their antioxidant activity are reported. Additionally, the growth-arresting effects of CURMs on A549 and HUVECs are studied to demonstrate their potential benefit in the treatment of cancer.

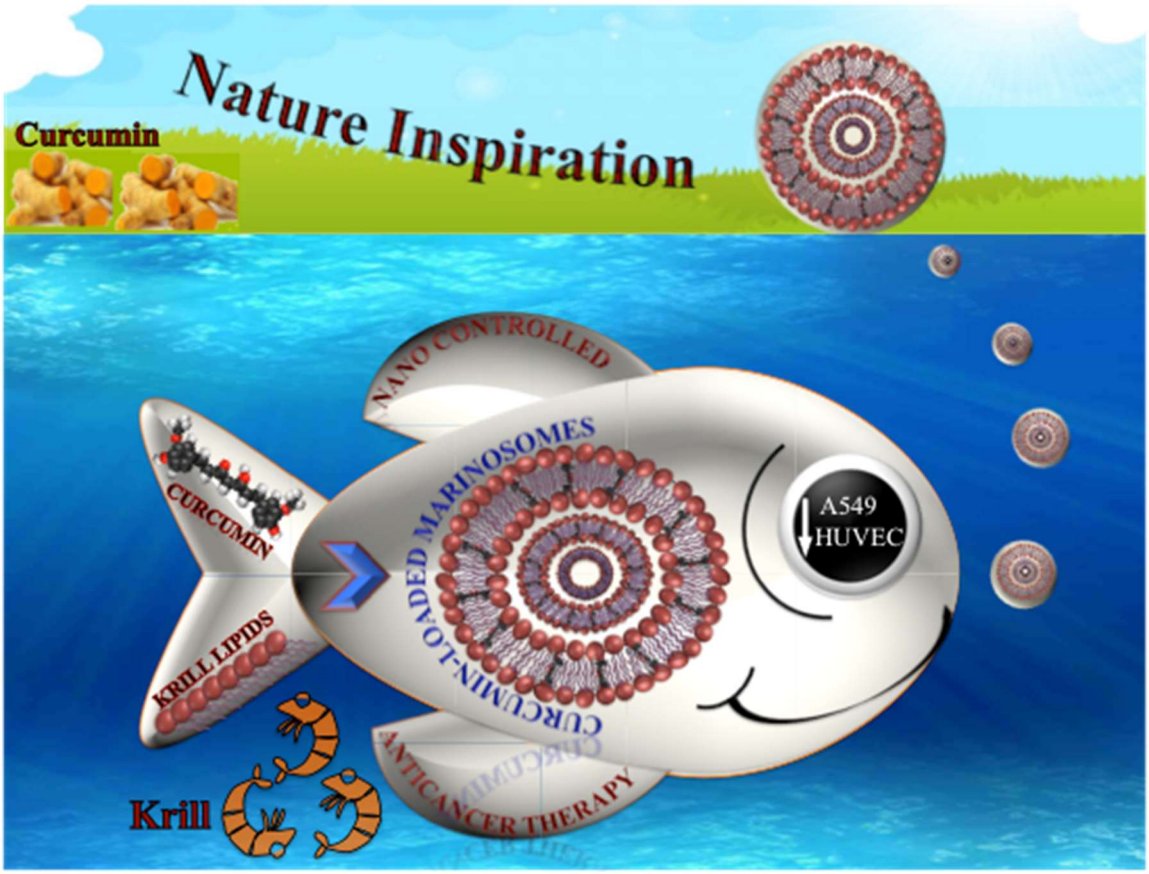

Fig. 19 Graphical abstract

The encapsulation of curcumin into krill lipid-based liposomes, which are readily available neutraceuticals to prepare nano controlled anticancer therapy, curcumin loaded marinosomes.

3.2. Materials and Methods

3.2.1 Materials

Curcumin was purchased from Sigma Aldrich. 2,2-diphenyl-l-picrylhydrazyl (DPPH) was purchased from Wako Pure Chemical (Osaka, Japan). Ethanol, chloroform and methanol were purchased from Wako Pure Chemical. PBS tablets were purchased from Takara Bio Inc. (Shiga, Japan).

The natural lipid mixture extracted from krill was supplied by Nippon Suisan company (Tokyo, Japan). The lipid extract analyzed by Japan Food Research Laboratories (Tokyo, Japan) contained the following weight percentages: saturated fatty acids (14.4 %), monounsaturated fatty acids (18.3 %), PUFAs (63.5 %), and inorganic metals, cholesterol, vitamin E, and dietary fibers (3.8 %). The fatty acids composition was determined using hydrogen flame ionization detection-gas chromatograph method. The polyunsaturated fatty acids were found to contain n-3 PUFAs (51.4 %) and n-6 PUFAs (3.1 %). The n-3 PUFAs were found to contain the following fatty acids: eicosapentaenoic acid (29.2 %; EPA (n-3)), docosahexaenoic acid (12.7 %: DHA (n-3)), octadecatetraenoic acid (3.7 % (n-3)) and docosapentaenoic acid (2.9 % (n-3)). The monounsaturated fatty acids were found to contain the following fatty acids: palmitoleic acid (9.2 % (n-7)), oleic acid (8.1 % (n-9)) and others (1 %). The saturated fatty acids were found to contain the following fatty acids: palmitic acid (7.5 %), myristic acid (5.6 %) and others (1.3 %).

3.2.2 Preparation of CURMs using the thin drug-lipid film hydration method

CURMs were prepared by reflux followed by thin drug-lipid film hydration method, which mentioned in details in chapter 2 with some modification. Krill lipids were taken with different weights (10, 15, 20, and 30 mg) in a glass bottle and dissolved in chloroform/methanol mixture (2/1, v/v). Curcumin (1 mg) was added to the lipid solution and the mixture was refluxed (tightly close the glass bottle and stir at a temperature of 50˚C for 2 h, **Fig. 20**). The resultant clear solution was evaporated to provide thin lipid films that were placed under high vacuum for at least overnight to remove the residual solvent. The dried drug-lipid film was hydrated in HBS to form MLVs. For the CURMs prepared using extrusion method, the MLVs were extruded 10 times through two Whatman Nucleopore Track-Etched polycarbonate membranes with 200 nm pores at 50˚C to decrease their sizes. For the CURMs prepared using sonication, the MLVs were sized using an ultra-sonic homogenizer (UH-50; SMT Company, Tokyo, Japan). The prepared formulations were cooled on ice for 15 min and unencapsulated curcumin was removed by centrifugation (1.5 X 10^3 g, 4˚C, 15 min). The mean size and polydispersity index (PDI) were determined using a dynamic light scattering instrument. Zeta potentials were measured using ZetaSizer Nano ZS90. The EE was calculated as described in **section 2.2.5**, but by absorbance at 425 nm.

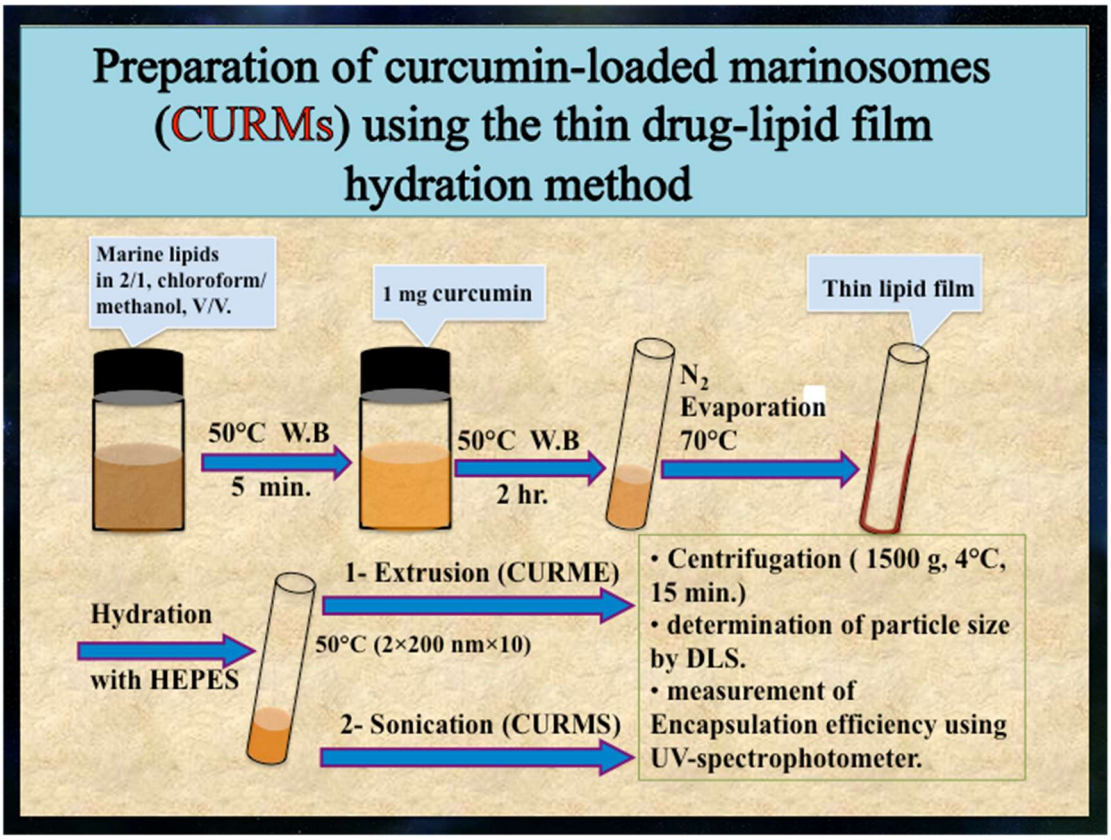

Fig. 20 Curcumin-loaded marinosomes preparation method

Curcumin was added to the lipid solution and the mixture was refluxed in water bath (W.B) and stir at a temperature of 50˚C for 2 h. After evaporation, hydration and extrusion, the particle size was determined using dynamic light scattering (DLS).

3.2.3 Determination of DPPH stability in detergent buffer solution

Method

The DPPH stability in detergent buffer solution was determined as previously reported after modification (Nicklisch and Waite, 2014). DPPH ethanolic solution at a concentration of 2 mM was freshly prepared in a glass bottle wrapped in aluminum foil to prevent photochemical decomposition. 1 ml of the 2 mM DPPH stock solution was added to 19 ml HBS treated with 0.3 % Triton X-100, the final concentration became 0.1 mM DPPH. The HBS-Triton mixture solution was wrapped in aluminum foil, mixed gently and incubated at room temperature in dark condition. In a spectrophotometer cuvette and after each predetermined time, a certain volume of HBS-Triton mixture was withdrawn and the absorbance was measured at 517 nm using a UV-visible spectrophotometer. A comparative study to prospect the capability of this HBS-Triton mixture to maintain the DPPH stability has been performed. The same method at the same conditions was repeated to measure the stability of DPPH in HBS buffer and methanol.

3.2.4 Determination of the antioxidant activity of CURMs in detergent buffer solution

The free radical scavenging activities of vitamin C, CURMs prepared by extrusion (CURME), CURMs prepared by sonication (CURMS), free curcumin and free marinosomes (FMs) were determined using DPPH assay as previously reported after modification (Aadinath et al., 2016). CURME, CURMS, and free curcumin were prepared with different concentrations ranging from 1.56 µg/ml to 25 µg/ml, added to different test tubes and adjusted to 950 µl using detergent buffer. Vitamin C as

positive control was dissolved in HBS buffer with concentration 1 mg/ml as a stock, and then different concentrations ranging from 1.56 μg/ml to 25 μg/ml were prepared using the detergent buffer. This detergent buffer is HBS treated 0.3 % Triton X-100 as previously reported after modification (Nicklisch and Waite, 2014). FMs were prepared at different concentrations of lipids ranging from 23.4 μg/ml to 375 μg/ml, which encapsulate the herein above-mentioned curcumin concentrations. Later 50 μl of 2 mM DPPH ethanolic solution was added to these tubes, the final concentration became 0.1 mM DPPH. The tubes were shaken and allowed to stand at room temperature for 40 min in dark condition. The control was prepared as mentioned above without the sample, and HBS-Triton mixture was used as a reference. A certain volume (230 μl/well) is transferred to 96-well plate and the absorbance was measured at 517 nm by using microplate reader (Wallac 4000 ARVO multi-label counter; PerkinElmer, Waltham, MA, USA). The antioxidant activity was calculated using the following formula:

Antioxidant activity % = (Abs control - Abs sample / Abs control) × 100

Where, *Abs control* and *Abs sample* are the absorbance values of the control and sample respectively. The EC_{50} values, which are the concentrations of samples required to obtain 50 % antioxidant activity, were determined based on the antioxidant activity curve using excel function tools.

3.2.5 Stability of CURMs under storage condition

CURMs were stored at 4˚C. As a typical experiment, the samples were centrifuged (1.5×10^3 g, 4˚C, 15 min) and aliquots were withdrawn at specified time points (0, 1, 2, 3, 4 ~ 8 weeks) as reported previously (Chen et al., 2015). Variations in the particle size, PDI and curcumin retention were measured. Additionally, the oxidative stability was determined following the same procedure mentioned in **section 3.2.4** The curcumin retention percentage was determined using spectrophotometer as described in **chapter 2,** and from the following equation as reported previously (Jin et al., 2016):

Curcumin retention %= (CUR Retained / CUR Encapsulated) × 100

Where *CUR Retained* is the amount of curcumin remained after the predetermined time and the *CUR Encapsulated* is the amount of curcumin that measured directly after preparation.

3.2.6 Retention of CURMs under culture condition

To test the retention of curcumin under *in vitro* culture conditions, a series of test tubes were prepared. In every test tube, 100 µl of CURMs was mixed with 100 µl of Dulbecco's Modified Eagle Medium (DMEM; Wako Pure Chemical) supplemented with 10 % heat-inactivated fetal bovine serum (Invitrogen, Carlsbad, CA, USA) and the samples were incubated at 37˚C in a humidified incubator in an atmosphere of 5 % CO_2/95 % air. The samples were centrifuged (1.5×10^3, 4˚C, 15 min), and the retention percentage was determined using spectrophotometer as described in **section 3.2.5.**

3.2.7 Cells

A549 cells were purchased from ATCC (Manassas, Virginia), maintained in DMEM, and supplemented with 10 % heat-inactivated fetal bovine serum, 100 U/ml penicillin and 100 μg/ml streptomycin. Primary HUVECs were purchased from Lonza (Basel, Switzerland), and cultured in endothelial cell basal medium-2 (Endothelial Basal Medium-2 (EBM-2; Lonza, cat. no. CC-3156). The cells were incubated at 37°C in a humidified incubator in an atmosphere of 5 % CO_2 / 95 % air.

3.2.8 Cytotoxicity study (WST Assay)

The cytotoxicity of the CURMS, free curcumin solution, and free marinosomes (FM) were evaluated using a Cell Counting Kit-8 (CCK-8; Dojindo, Kumamoto, Japan) as previously described after modification (Tagami et al., 2015). Briefly, A549 and HUVEC cells were prepared in medium, and seeded into 96-well cell incubation plate at a density of 5.0×10^3 cells/well. A549 were pre-incubated for 48 h and then treated with different concentrations (0, 10, 20, 30, 40 μg/ml) of CURMS. In addition, the cells were treated with free curcumin, as a positive control, that was dissolved in ethanol and diluted by medium to the desired concentrations (0, 10, 20, 30, 40 μg/ml) as previously reported after modification (Tagami et al., 2014), where the final ethanol concentration is kept under 0.5 %. Furthermore, the cells were treated with FMS prepared with different concentrations of lipids (0, 150, 300, 450, 600 μg/ml) that encapsulate the herein above-mentioned concentrations of curcumin. Regarding to HUVEC, the cells were incubated with different concentrations (0, 1.56, 3.12, 6.25, 12.5 μg/ml) of CURMS and free curcumin. The cells were also treated with FMS prepared with different concentrations of lipids (0, 23.4, 46.8, 93.8, 188

μg/ml) that encapsulate the specified concentrations of curcumin. After exposure to the drug for predetermined time intervals (24, 48, 72 hours) the cells were washed with PBS. The PBS was aspirated and then 110 μl of the solution mixture (100 μl medium and 10 μl of CCK-8 solution) was added to the wells. After A549 cells were incubated for 1 hour and HUVEC cells were incubated for 4 hours, the absorbance was measured using microplate reader at 450 nm. The cell viability and cytotoxicity were calculated after subtraction of the background absorbance of the medium from the total absorbance using the following equations:

Cell viability %= (Experimental Abs / Control Abs) × 100

Where *Experimental Abs* is the absorbance of the wells treated with different concentrations of the drug and *Control Abs* is the absorbance of the wells incubated only with medium. The IC_{50} value, which is the half maximal inhibitory concentration, was calculated through linear and nonlinear curve fitting that performed using excel function tools.

3.2.9 Statistical Analysis

All data shown here are represented in "mean value ± S.D.". The two-way ANOVA, with Bonferroni multiple comparison test, was used to assess statistical significance by using GraphPad Prism (GraphPad Software Inc., CA, USA).

3.3. Results and discussion

3.3.1 CURMs prepared using the thin drug-lipid film hydration method

Krill lipids extract was reported to be the leading marine phospholipid product on the market with approximately 35 % phospholipid (Neptune Technologies & Bioressources, 2001). In addition, It was reported that almost half the lipid content of Krill presents in a phospholipid form, mainly phosphatidylcholine (Castro-Gómez et al., 2015). Phospholipid has a special molecular structure, which contains both hydrophilic head group and lipophilic fatty acid group. Subsequently, phospholipids have a good emulsifying properties and could be used as natural surfactants to prepare emulsion without addition of other emulsifiers (Lu et al., 2012). Additionally, it was reported that the marine extracted lipids have a potential oxidative stability to prepare liposomes (Lu et al., 2011). Consequently, in the present study the preparation of marinosomes from krill lipid extract and the loading of curcumin at reasonable drug-to-lipid ratios are accomplished. CURMs were prepared by incorporating the drug into the lipid phase using the thin drug-lipid film method after refluxing the drug with the lipids for 2 hours. CURMs have liposome-like vesicle structure because of self-assembly property of phospholipids molecules. In reflux, it seems that raising the temperature melted the lipids and led to dissolve the curcumin into the lipid phase (Maiti et al., 2007). Additionally, curcumin could undergo hydrophobic interaction through its aromatic rings and hydrogen bonding through its phenol rings (Began et al., 1999). Therefore, the encapsulation efficiency of curcumin into the lipid phase increased. As shown in **Table 4**, the four formulations of CURM and FM prepared by extrusion (FME and CURME) in this experiment have uniform sizes. The values of

the particle size of FME, CURME 10, CURME 15, CURME 20 and CURME 30 are 118 ± 4, 120 ± 6, 105 ± 8, 101 ± 7 and 120 ± 4, respectively. The zeta potential values are ranging from -13 ± 2 mV to -15 ± 1 mV. The particle size distribution of FME and CURME has a single peak, as shown in **Fig. 21A and B**, with a narrow size distribution (PDI < 0.12). However, as shown in **Table 5**, the four formulations of CURMs and FMs prepared by sonication method (CURMS and FMS) have uniform sizes. The values of the particle size of FMS, CURMS 10, CURMS 15, CURMS 20 and CURMS 30 are 63 ± 2, 94 ± 4, 81 ± 3, 63 ± 2 and 60 ± 3, respectively. Furthermore, The zeta potential values are ranging from -13 ± 1 mV to -15 ± 2 mV. The particle size distribution of FMS and CURMS has a single peak, as shown in **Fig. 21C and D**, with a slightly wider size distribution (PDI < 0.27) compared to that of FME and CURME. In the extrusion method, increasing the lipid/curcumin ratio does not show significant effects on particle size, PDI, and zeta potential, as shown in **Table 4**. This is not surprising, as it is well known that the extruded vesicles would be close in diameter to the pore size of the polycarbonate membranes used to prepare them (MacDonald et al., 1991). Additionally, the difference in the particle size between CURME 15 and FME is likely due to the variability of manual pressure applied during the extrusion. Particularly, CURME 10 and FME have nearly similar particle sizes. However, in sonication method the lipid/curcumin ratio affects the particle size of CURMS, as shown in **Table 5**. As the lipid/curcumin ratio increases from 10/1 to 30/1 the particle size decreases from 94 ± 4 to 60 ± 3 nm, respectively, in agreement with what is previously reported (Anuchapreeda et al., 2011). In **Table 5**, it is worthy to note that there is a clear difference in particle size between FMS and CURMS 15 (63 ± 2 nm and 81 ± 3 nm, respectively). This could be due to the

incorporation of curcumin in the lipid layer of the liposomes. The negative charge of zeta potential values, shown in **Table 5**, could be due to the partition of the negatively charged phospholipids and free fatty acids into the lipid layer.

Lipid weight (mg/ml)	Particle size (nm)	Polydispersity index	Zeta potential (mV)
15 (FME)	118 ± 4	0.09 ± 0.02	-15 ± 1
10	120 ± 6	0.06 ± 0.02	-13 ± 2
15	105 ± 8	0.10 ± 0.02	-14 ± 2
20	101 ± 7	0.12 ± 0.01	-14 ± 1
30	120 ± 4	0.12 ± 0.02	-14 ± 1

Table 4. FM and CURM prepared by extrusion method (FME and CURME)

CURME prepared by addition of 1 mg curcumin to different weights of lipids (10, 15, 20, and 30 mg). FME is free marinosomes prepared with lipid weight = 15 mg/ml. Data represent the means ± S.D. (n = 3).

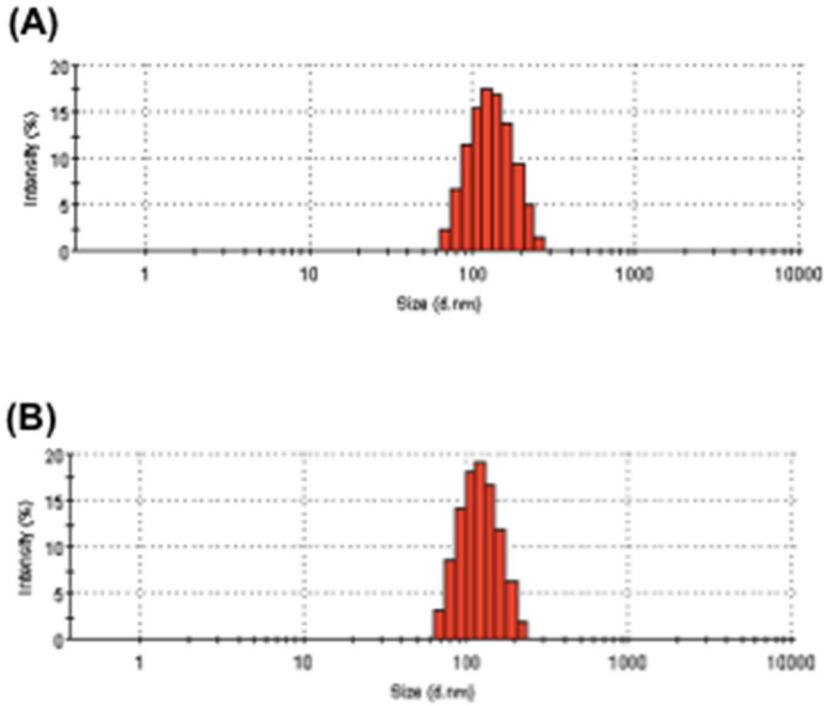

Fig. 21. DLS measurements of (A) free marinosomes (FME) prepared using extrusion method and (B) curcumin-loaded marinosomes (CURME) prepared using extrusion method. The CURME formulations were prepared, at lipid/drug ratio of 15/1 w/w, and FME formulations were prepared at lipid concentration = 15 mg/ml. The information about PDI and zeta potential are written in Table 4.

Lipid weight (mg/ml)	Particle size (nm)	Polydispersity index	Zeta potential (mV)
15 (FMS)	63 ± 2	0.27 ± 0.01	-15 ± 2
10	94 ± 4	0.07 ± 0.01	-15 ± 1
15	81 ± 3	0.16 ± 0.02	-13 ± 1
20	63 ± 2	0.26 ± 0.01	-14 ± 1
30	60 ± 3	0.26 ± 0.01	-15 ± 1

Table 5. FM and CURM prepared by sonication method (FMS and CURMS)

CURMS prepared by addition of 1 mg CUR to different weights of lipids (10, 15, 20, and 30 mg). FMS is free marinosomes prepared with lipid weight = 15 mg/ml. Data represent the means ± S.D. (n = 3).

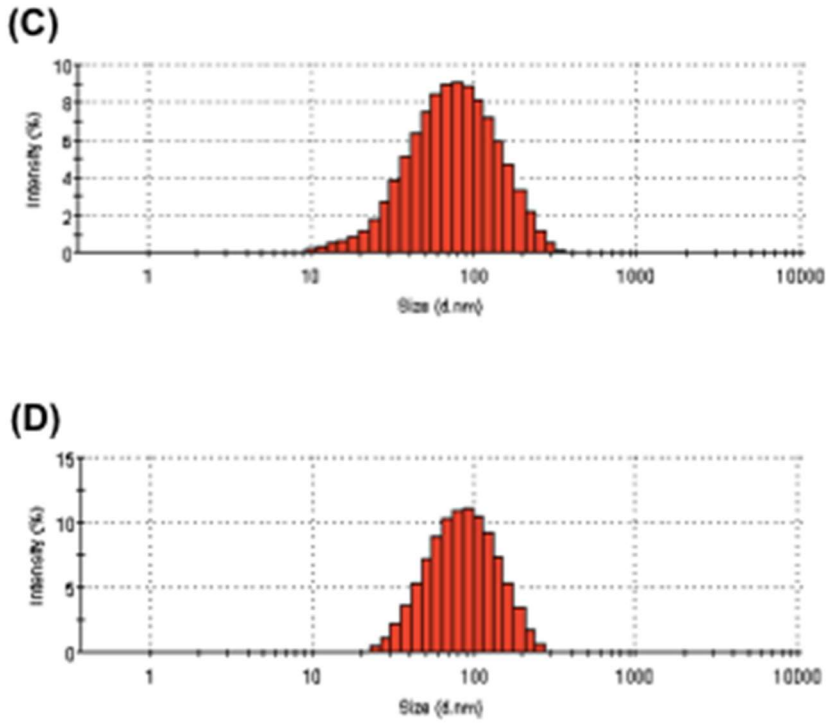

Fig. 21. DLS measurements of (C) free marinosomes (FMS) prepared using sonication method and (D) curcumin-loaded marinosomes (CURMS) prepared using sonication method. The CURMS formulations were prepared, at lipid/drug ratio of 15/1 w/w, and FMS formulations were prepared at lipid concentration = 15 mg/ml. The information about PDI and zeta potential are written in Table 5.

3.3.2 EE of CURMs

The EE measurement of CURMs reveals that the EE increases with the increase of lipid concentration up to 15 mg and saturated beyond this level as most of the added curcumin amount (1 mg) has been encapsulated, shown in **Fig. 22**. Additionally, the slight decrease in the EE of CURME at high lipid concentration (30

mg) could be due to the entrapment of a slight amount of lipids between the two-polycarbonate membranes during the extrusion method. Particularly, using sonication method didn't show that decrease in the EE of the CURMS at the same high concentration. In a preliminary experiment, 40 mg amount of lipids was used to encapsulate the same amount of curcumin resulted in further decrease in the EE which confirm the previous observation. Additionally, the sonication and the extrusion methods resulted in almost the same EE. When the CURMs were centrifuged to separate the excess curcumin after preparation, pellets of excess curcumin were seen only at low lipid weight (10 mg).

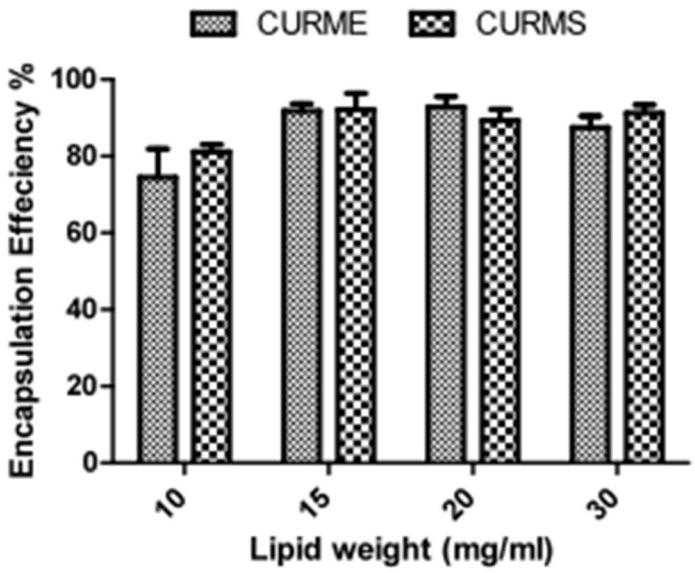

Fig. 22. The encapsulation efficiency (EE) of CURMs prepared using extrusion (CURME), and sonication (CURMS). Four formulations were prepared at lipid/curcumin ratios of 10/1, 15/1, 20/1, and 30/1 (w/w). Data represent the means ± S.D. (n = 3). No significant differences ($p > 0.05$) between CURME and CURMS.

3.3.3 Determination of the antioxidant activity of CURMs in detergent buffer

In food and biological extracts, the standard DPPH assay is accustomed to be used for the *in vitro* determination of antioxidant activity (Prior et al., 2005). The interaction kinetics of DPPH assay with polyphenolic and non-phenolic compounds have been recently well studied (Villaño et al., 2007). In case of curcumin, DPPH scavenging is accelerated by hydrogen atom transfer or sequential proton loss electron transfer mechanism (Feng and Liu, 2009). However, it is well known that the DPPH assay uses methanol, ethanol or buffered alcoholic to keep the DPPH soluble for the *in vitro* determination of antioxidant activity. The DPPH scavenging activity of CURMs has to be tested in buffer to mimic the *in vivo* environment, while the DPPH is insoluble and unstable in buffer solutions. In the present study, a simple *in vitro* method to measure the antioxidant activity of liposomal formulations in buffer is used following a recent report after modification (Nicklisch and Waite, 2014). In a preliminary experiment, 0.3 % Triton X-100 was selected to keep 100 μM DPPH soluble and stable in HBS buffer for up to 40 min, which is the needed time to measure the antioxidant activity. The absorbance of DPPH in the HBS-Triton mixture is reduced to 80 % after 180 min, shown in **section 3.2.3 and Fig. 23**. If more time is needed, other detergents or buffers have to be tested first. The surfactant molecules form micelles at critical micelle concentration, this could help to dissolve and stabilize the hydrophobic molecules that are sparingly soluble in aqueous solutions. After determination of the antioxidant activity of ascorbic acid as a positive control using HBS-Triton mixture, shown in **Table 6**, we found that EC_{50} values agree with what was reported previously using methanol or buffered methanol solution (Sharma

and Bhat, 2009). In **Fig. 24,** increasing the sample concentration resulted in increasing the antioxidant activity, which reveals a dose-dependent antioxidant activity. CURME and CURMS showed strong DPPH radical scavenging abilities. The antioxidant activities (at 25 μg/ml) of CURME and CURMS are 91.1 % ± 0.3 % and 89.5 % ± 2.5 %, respectively, that are as high as that of vitamin C (82.9 % ± 5.8 %) and clearly higher than that of curcumin (69.8 % ± 7.6 %). This indicates that CURMs possibly react, as electron donors, with free radicals and thus convert them into more stable compounds and stop further radical reactions.

In addition, the EC_{50} values of CURME and CURMS are 4.0 ± 0.9 μg/ml and 4.3 ± 1.8 μg/ml, respectively, which are nearly similar to that of vitamin C (4.5 ± 1.1 μg/ml) and significantly lower than that of curcumin (13.6 ± 2.8 μg/ml), shown in **Table 6**. Furthermore, the curve of the antioxidant activity of CURMs reached nearly a stationary phase at a relatively low concentration (12.5 μg/ml). Consequently, CURMs could be considered as powerful antioxidants with a very high reactivity with free radicals. A synergistic antioxidant effect of phospholipid on α-tocopherol was previously reported (Cho et al., 2001; Moriya et al., 2007). Subsequently, the increasing of the CURMs antioxidant activity compared to free curcumin could be explained due to a presumably synergistic antioxidant effect of phospholipid on curcumin.

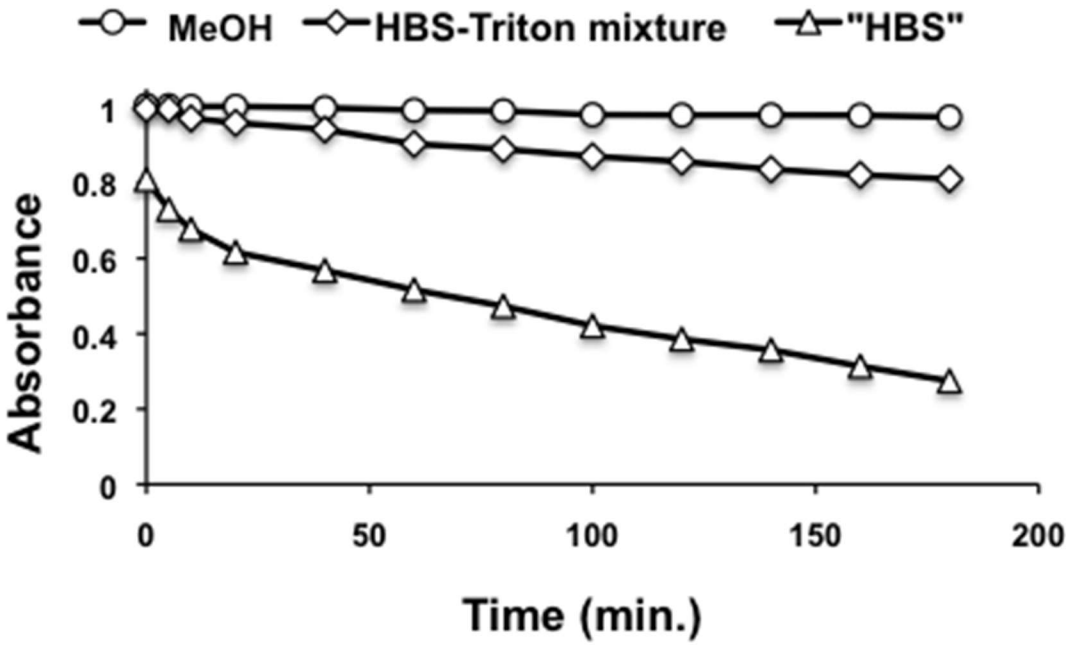

Fig. 23. Time course stability of DPPH in methanol, HBS-Triton mixture and HBS buffer at room temperature.

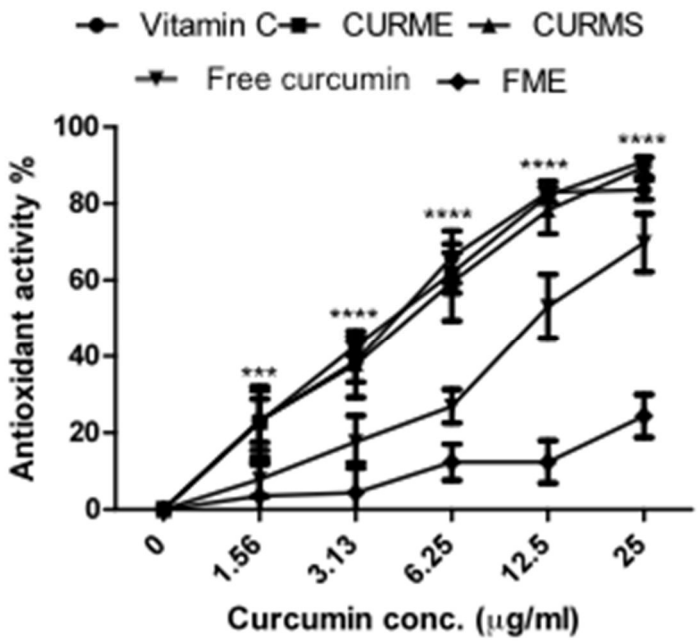

Fig. 24. The antioxidant activity of CURME, CURMS, free curcumin and FME in HBS-Triton mixture using DPPH assay. CURMs were prepared at lipid/curcumin ratio of 15/1 (w/w). FM is prepared at lipid concentration = 15 mg/ml. CURME, CURMS, free curcumin, and Vitamin C were prepared with different concentrations ranging from 1.56 µg/ml to 25 µg/ml. FME were prepared at different concentrations of lipids ranging from 23.4 µg/ml to 375 µg/ml, which encapsulate the herein above-mentioned curcumin concentrations. Data represent the means ± S.D. (n = 6). No significant differences ($p > 0.05$) between CURMs and vitamin C. (***) Significant difference ($p < 0.001$) and (****) significant differences ($p < 0.0001$) compared to free curcumin.

Sample	EC_{50}	EC_{50}
Vitamin C	25.6 ± 6.2 µM	4.5 ± 1.1 µg/ml
CURME	10.9 ± 2.4 µM	4.0 ± 0.9 µg/ml
CURMS	11.7 ± 4.9 µM	4.3 ± 1.8 µg/ml
Free curcumin	36.9 ± 7.6 µM	13.6 ± 2.8 µg/ml
FME		1.01 ± 0.11 mg/ml

Table 6. EC_{50} of a maximum scavenging activity of CURMs

EC_{50} of CURME, CURMS, free curcumin and FME using DPPH assay, as shown in Figure 24. Data represent the means ± S.D. (n = 3).

3.3.4 Stability of CURMs under storage condition

Physical instability leads to fusion of vesicles or leakage of the encapsulated drug. Additionally, curcumin undergoes fast hydrolytic degradation under basic and neutral pH conditions, which results in low pharmacological activities (Chen et al., 2015). Therefore, the storage stability is an important issue for drug delivery formulations. In the present study, the physical stability of CURME, CURMS and FME including particle size, PDI, and curcumin retention was investigated. Additionally, since the antioxidant capacity and free radical scavenging ability could be gradually lost during the storage, they have to be measured during and after the storage period. CURME, CURMS, and FME (lipid/drug ratio 15/1 w/w) were stored at 4˚C for eight weeks. **Fig. 25A** and **25B** reveal that the mean particle diameter and PDI of CURME, CURMS and FME did not change significantly during 8 weeks. **Fig. 25C** shows that the retention rate of curcumin in CURME and CURMS slightly decreased to 89.5 ± 2.5 % and 92.7 ± 1.9 % of their initial values, respectively, after storage of 8 weeks. Additionally, no significant change in the antioxidant activity of CURME, CURMS, and FME (91.7 ± 0.13, 91.8 ± 0.18 and 26.8 ± 1.4, respectively) after storage of 6 weeks at 4˚C as shown in **Fig. 25D**. However, the oxidative stability of CURME and CURMS slightly decreased to 78.7 ± 2.5 % and 79.0 ± 2.7 %, respectively, after storage of 8 weeks. This decrease could be due to the decrease in the retained curcumin amount (about 10 %, shown in **Fig. 25C**) after storage of 8 weeks. Particularly, the oxidative stability of FME shows no significant change after storage of 8 weeks. This could imply the utility of marinosomes to incorporate hydrophobic drugs and CURMs possess a favorable physical stability when stored at

4 °C. The physical stability of marine liposomes may be attributed to four different factors. The first, the storage at low temperature (4°C) inhibits the membrane fluidity of the nanoliposomes The second, the presence of cholesterol in marine lipids may increase the rigidity of marinosomes due to the resistance of cholesterol-incorporated liposome toward degradation (Grit et al., 1993). The third, the negative charges of phospholipids contribute to electrostatic stability (Lu et al., 2012). The fourth, the presence of free fatty acids in the marine lipids and their distribution in the lipid layer of marinosomes increase the negative surface charge in agreement with a previous report which showed that the the incorporation of alkali fatty acids with phospholipid had a positive influence on the surface charge of O/W emulsion (Buszello et al., 2000). Additionally, the oxidative stability of marine liposomes could be attributed to three different factors. The first, the presence of PUFAs in the sn-2 position of the phospholipids may forbid oxygen and free radicals to attack PUFAs due to this tightly packed molecular conformation (Applegate and Glomset, 1986). The second, the presence of other antioxidant compounds like astaxanthin and α-tocopherol that are potent antioxidants (Castro-Gómez et al., 2015). The third, the presumably synergistic antioxidant effect of phospholipid and α-tocopherol (Cho et al., 2001).

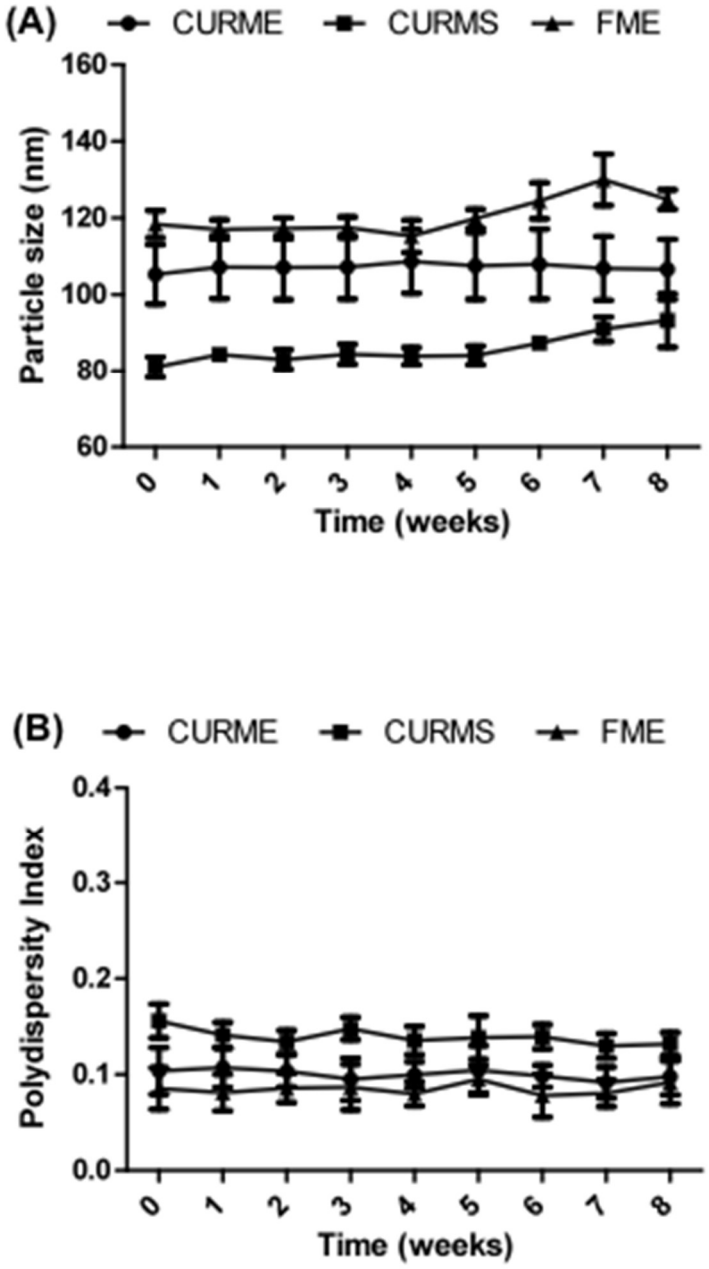

Fig. 25. Stability of CURME, CURMS and FME during storage at 4°C for 8 weeks. CURMs were prepared at lipid/curcumin ratio of 15/1 (w/w). FM is prepared at lipid concentration = 15 mg/ml. A) Particle size. B) PDI. Data represent the means ± S.D. (n = 3).

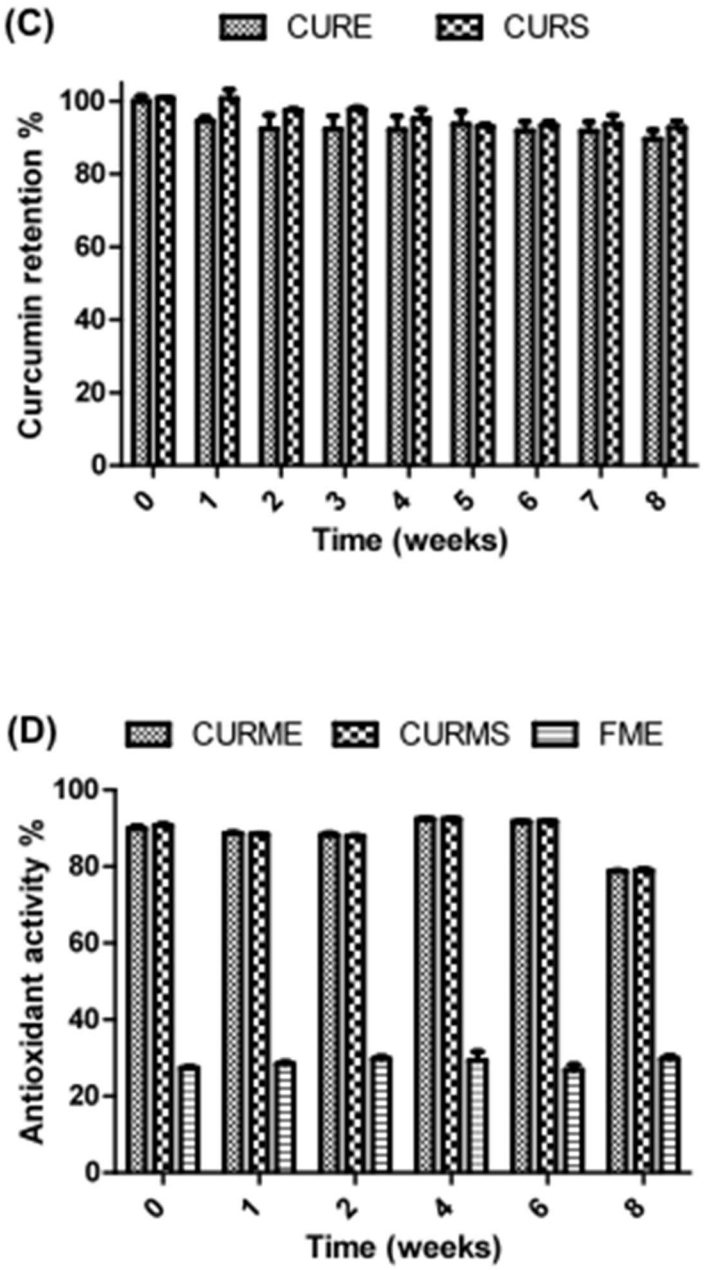

Fig. 25. Stability of CURME, CURMS and FME during storage at 4°C for 8 weeks. CURMs were prepared at lipid/curcumin ratio of 15/1 (w/w). FM is prepared at lipid concentration = 15 mg/ml. C) Curcumin retention %. D) Oxidative stability. Data represent the means ± S.D. (n = 3).

3.3.5 Retention of curcumin into marinosomes under cell culture condition

A drug release study was carried out in a medium containing fetal bovine serum to mimic i*n vivo* conditions. In the present study, because of the curcumin hydrolytic degradation, curcumin retention has been measured instead of drug release measurements to study the *in vitro* drug release. In case of CURMs (lipid/drug ratio of 15/1 w/w), curcumin retention undergoes initial decrease to reach 80.5 ± 5.5 % (CURME) and 88.8 ± 7.9 % (CURMS) of its initial value after 4 hours as shown in **Fig. 26**. Afterward the curcumin retention continued in gradual decrease to 70.1 ± 5.2 % (CURME) and 75.6 ± 1.1 % (CURMS) during 72 hours. The reason behind the high decrease rate of curcumin retention during the early stage of the measurement (~ 4 hours) is possibly the adsorption of some drug molecules on the surface of CURMs during the thin film preparation. It is well known that increasing the content of PUFA leads to increasing the fluidity of liposomes under physiological conditions compared to that of the saturated lipids (Saiz and Klein, 2001). Krill lipid is a mixture of saturated fatty acids, monounsaturated fatty acids, poly-unsaturated fatty acids, cholesterol and others as mentioned in **section 3.2.1**. In addition, nearly half of the PUFAs of krill lipid are located in phospholipids (mainly phosphatidyl-choline) as it is previously reported (Castro-Gómez et al., 2015; Lu et al., 2011). Consequently, increasing the temperature to body temperature leads to increase the fluidity of marinosomes due to the presence of PUFAs and thus the curcumin release starts. However the presence of saturated fatty acids, phospholipids and cholesterol in krill lipid prevents marinosomes from complete fluidity and thus resulted in a controlled release phenomenon. The drug release is sustainable (0 - 30 % at 0 - 72 hours), shown

in **Fig. 26**, denoting the significance of marinosomes as a drug delivery system. It is possible that 30 % of the drug undergoes burst release and controlled release from the outer layer of the marinosomes. This result opens the door widely to the *in vitro* anticancer experiment to thoroughly investigate the controlled release of these formulations as discussed herein after.

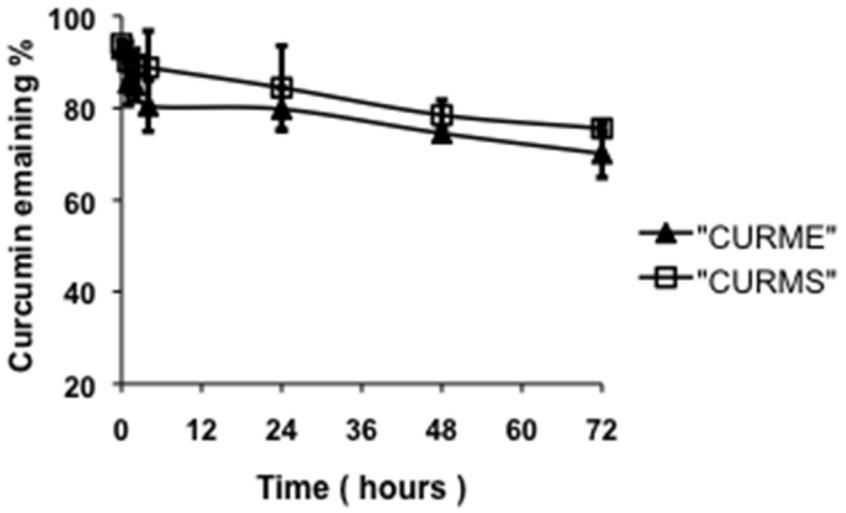

Fig. 26. Retention of curcumin into marinosomes under culture condition. CURME and CURMS were prepared at lipid/curcumin ratio of 15/1 (w/w). FM is prepared at lipid concentration = 15 mg/ml. CURMs were incubated in medium containing 10 % fetal bovine serum at 37˚C. Data represent the means ± S.D. (n = 3).

3.3.6 The cytotoxicity of free and curcumin-loaded marinosomes on A549 cells:

A comparative cytotoxicity study to prospect the capability of CURMS to deliver highly hydrophobic drugs such as curcumin to lung cancer cells has been performed. A549 cells were treated separately with free curcumin as drug solution, CURMS and FMS for different times and concentrations. The effect of controlled release of curcumin under culture condition (**section 3.3.5.**) was confirmed when cancer cells were used.

Fig. 27A shows cytotoxicity after incubation with A549 cells for 24 hours, free curcumin has a cytotoxic effect of 63.4 ± 6.5 % (the highest) while CURMS shows only 10.9 ± 5.9 % at 20 μg/ml of curcumin concentration. At incubation time equal to 48 hours, free curcumin and CURMS show nearly the same cytotoxic effect of 59.3 ± 4.0 % and 55.7 ± 2.5 % at 20 μg/ml, respectively, shown in **Fig. 27B**. However, when the incubation time is extended to 72 hours, the cytotoxic effect of CURMS increased to 90.9 ± 2.2 % (the highest) and that of free curcumin decreased to 45.7 ± 9.2 % at the same curcumin concentration (20 μg/ml) as clearly shown in **Fig. 27C**. The IC_{50} values of free curcumin are 14.3 ± 5.1, 18.2 ± 2.9 and 19.8 ± 2.3 μg/ml at 24, 48 and 72 hours, respectively, stated in **Table 7**. This means that free curcumin gives its ultimate effect on the cell during the early stage of the experiment and this may be due to the passive diffusion and accumulation of curcumin directly at its action site (Mohanty et al., 2010). While the IC_{50} values of CURMS are 35.0 ± 1.1, 19.9 ± 1.03 and 11.7 ± 0.24 μg/ml at 24, 48 and 72 hours, respectively. This result clearly indicates the sustained release of curcumin from marinosomes over time that agrees with previous reports (Ma et al., 2007; Mohanty et al., 2010). It is worthy to

notice that the cytotoxic effect of FMs is only clear at higher marinosomal doses (450 and 600 μg/ml) in a time- and dose-dependent manner.

It has been reported that PUFAs are taken up by tumors for use as precursors for biochemical metabolic pathways and energy production (Sauer and Dauchy, 1992). Once taken up, they are incorporated in the cellular membranes of the tumor and contribute to membrane fluidity, ion permeability and elasticity (Merendino et al., 2013). Plasma membrane is composed of microdomains that include structures known as lipid rafts and caveolae, which are rich in cholesterol and sphingolipids, and play a key role in cell signal transduction (Ma et al., 2004). The inclusion of n-3 PUFAs in tumor cell membranes, especially microdomains, may affect physicochemical properties of membranes due to their high unsaturation. This could explain the capability of n-3 PUFAs to induce cytotoxic effect in tumor cells through the regulation of multiple cellular functions (D'Eliseo and Velotti, 2016). This unique property of tumor biochemistry or physiology could be used to target tumors and increase the therapeutic effect of a chemotherapy with less side effect (Bradley et al., 2001; Kuznetsova et al., 2006).

It was reported that at a relatively high concentration (above 15 μg/ml) of curcumin-loaded micelles, the cytotoxic effect was reduced due to saturation of the endocytic process which resulted in reduced drug entry (Ma et al., 2007; Mohanty et al., 2010). However, the current study shows that the cytotoxicity of CURMS at such high concentrations increases in a time dependent manner. The cytotoxicity of CURMS at 30 and 40 μg/ml is 96.6 ± 0.2 %, and 96.6 ± 0.2 % after 72 hours. This could be due to the affinity of PUFAs to microdomains that may lead to incorporation of the marinosomes into the plasma membrane and enhance the internalization of

curcumin. Additionally, A549 cells were reported to employ multiple endocytotic pathways (Kuhn et al., 2014) that possibly localize CURMs in intracellular vesicles. Afterword, a gradual release of curcumin from CURMs occurred resulted in a controlled release of curcumin.

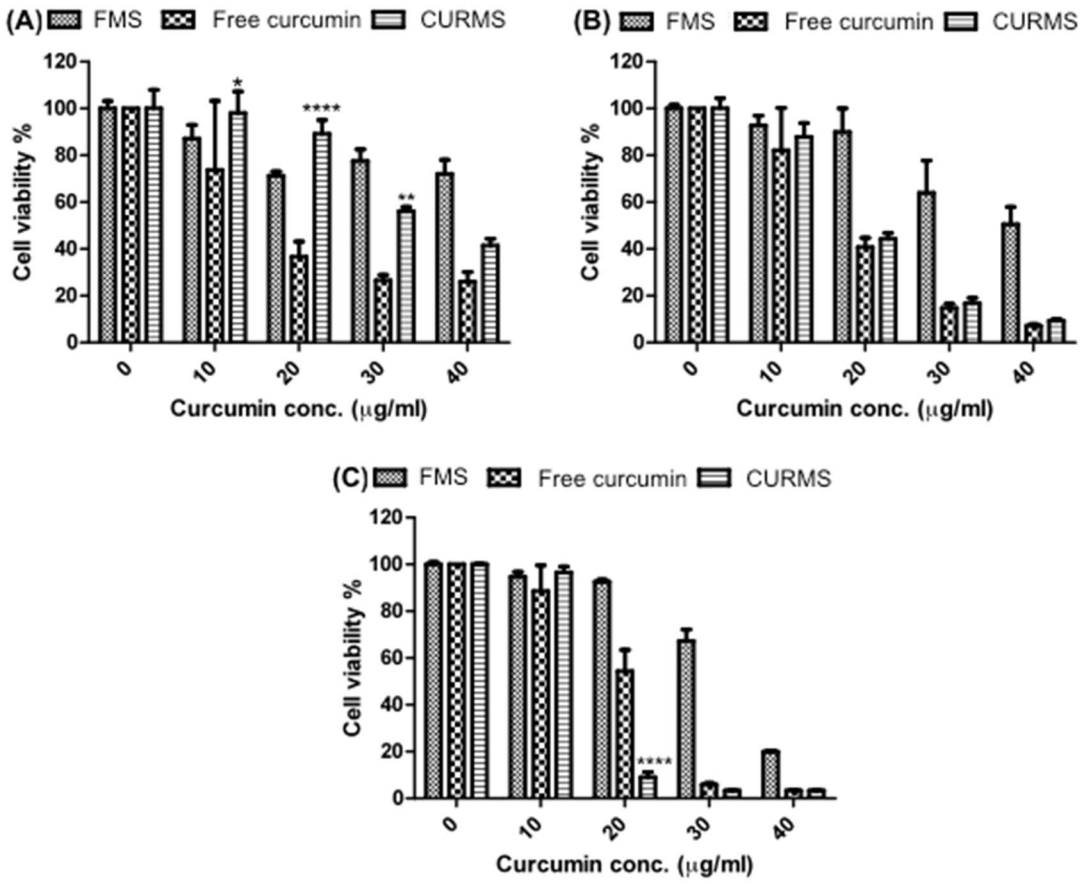

Fig. 27. *In vitro* cytotoxic effect of CURMS and FMS on A549 lung cancer cells.

The cells were treated with CURMS, free curcumin, and FMS. CURMS were prepared by sonication at lipid/curcumin ratio of 15/1 (w/w). FMS is prepared at lipid concentration = 15 mg/ml. (A) After incubation for 24 hours, (B) After incubation for 48 hours and (C) After incubation for 72 hours. Data represent the means ± S.D. (n = 3). There is (*) Significant difference ($p < 0.05$), (**) significant differences ($p < 0.01$) and (****) significant differences ($p < 0.0001$) between CURMS and free curcumin.

Cell line	CURMS (µg/ml)	Free curcumin (µg/ml)	FMS (µg/ml)
A549 (24 hours)	35.0 ± 1.1	14.3 ± 5.1	NA
A549 (48 hours)	19.9 ± 1.0	18.2 ± 2.9	586.0 ± 66.6
A549 (72 hours)	11.7 ± 0.2	19.8 ± 2.3	485.4 ± 9.3
HUVEC (24 hours)	2.64 ± 0.2	5.73 ± 2.1	NA
HUVEC (48 hours)	2.95 ± 0.2	10.3 ± 4.4	NA
HUVEC (72 hours)	2.97 ± 0.0	9.09 ± 2.7	NA

Table 7. IC_{50} values of CURMS, free curcumin and FMS against A549 lung cancer cells and HUVEC cell line.

Both cell lines were assayed for cell viability by WST-assay at 24 hours, 48 hours and 72 hours as shown in Fig. 27 and Fig 28. The IC_{50} values were calculated using excel function tools. NA is the non-available IC_{50} values of FMS as their concentrations were not enough to reach 50 % cytotoxic effect in the present study. Data represent the means ± S.D. (n = 3).

3.4.7 The effect of free and curcumin-loaded marinosomes on HUVECs

The formation of new blood vessels is a natural process called angiogenesis and it is essential during wound healing and embryonic development (Madri et al., 1991). However, many pathologies, including tumor growth, are arising from uncontrolled angiogenesis (Carmeliet et al., 2003). Endothelial cells are among the essential cells that constitute the dynamic environment of tumors as they form the blood vessels. It was reported that curcumin is able to inhibit the proliferation of HUVECs and act as anti-angiogenic compound (Thaloor et al., 1998). In addition, it was reported that n-3 PUFAs have anti-angiogenic effect (Szymczak et al., 2008). Consequently, the time- and dose-response of CURMS, FMS and free curcumin on HUVEC growth were investigated in the present study. CURMS inhibited the proliferation of HUVECs in a dose-dependent manner as shown in **Fig. 28**. The highest cytotoxic effect of CURMS and free curcumin were observed at 6.25 μg/ml after 24 hours (85.2 ± 1.1 % and 50.2 ± 4.5 %, respectively), shown in **Fig. 28A**. Additionally, The IC_{50} values of CURMS and free curcumin at 24 hours are (2.64 ± 0.21, 5.73 ± 2.1 μg/ml, respectively, shown in **Table 7**. The highest cytotoxic effect of FMS is (44.7 ± 8.7 %) at concentration of 188 μg/ml after 48 hours, and this could be due to the low concentrations of lipids that were used in this experiment.

The trends of the cytotoxic effects of CURMS, shown in **Fig. 28**, don't indicate obvious change in the cell viability after incubation for more than 24 hours (**Fig. 28B and C**), and thus no controlled release has been observed in this case. It was reported that the cellular membrane of endothelial cells is high in caveolae (Cohen et al., 2004) and that HUVEC cells express more caveolins than others (Voigt

et al., 2014). This observation is previously used to target HUVEC cells using negatively charged lipid nanoparticles, without the need for cell-specific targeting ligands, depending on the high affinity of the lipophilic nanoparticles for caveolae (Voigt et al., 2014). This could lead to a high incorporation of CURMS into caveolae and a fast release of curcumin inside the HUVEC cells, and thus the ultimate cytotoxic effect occurred directly after incubation for 24 hours. However, further experiments to determine the uptake pathways of A549 and HUVEC cells for CURMs are considered to be future aspects of study.

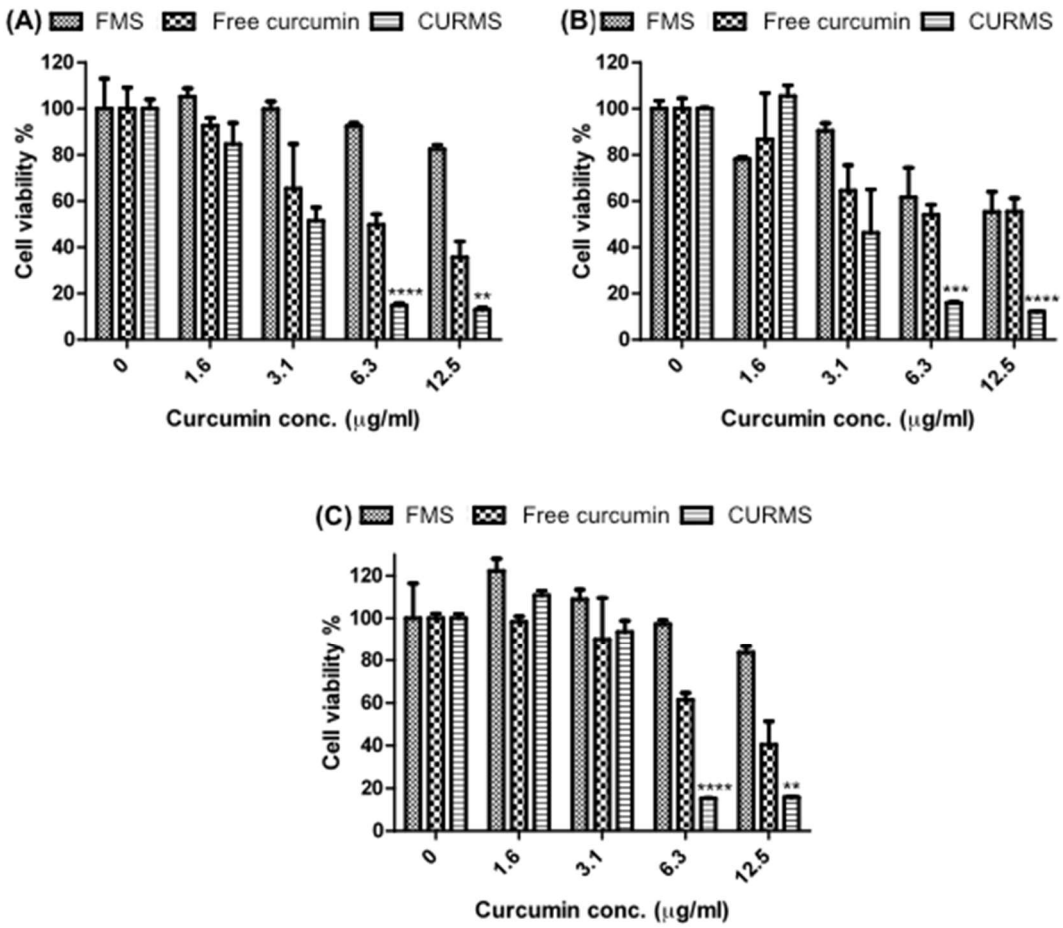

Fig. 28. *In vitro* cytotoxic effect of marinosomes on HUVEC cell line. The cells were treated with CURMS, free curcumin, and FMS. CURMS were prepared by sonication at lipid/curcumin ratio of 15/1 (w/w). FM is prepared at lipid concentration = 15 mg/ml. (A) After incubation for 24 hours, (B) After incubation for 48 hours and (C) After incubation for 72 hours. Data represent the means ± S.D. (n = 3). There is (**) significant differences ($p < 0.01$), (***) significant differences ($p < 0.001$) and (****) significant differences ($p < 0.0001$) between CURMS and free curcumin.

3.5. Conclusion

The present study exhibits the encapsulation of curcumin into krill lipid-based liposomes through utilizing a modified thin drug-lipid film hydration method followed by extrusion or sonication. CURMs of uniform diameter, and narrow PDI were prepared with high encapsulation efficiency (92.0 ± 5.9 %) at a lipid/drug ratio of 15/1 (w/w). This approach resulted liposomal formulations of high physicochemical and oxidative stability. The krill lipids-based curcumin-loaded liposomes prepared in this study exhibited an effective cytotoxic effect after 72 hours on A549 cells due to the controlled release phenomenon and after 24 hours on HUVEC cells. These nano-nutraceutical liposomal formulations represent low-cost drug delivery systems that could be applied for efficient solubilization, stabilization and controlled delivery of the biological active and hydrophobic compounds for cancer and other inflammatory diseases targeting. However, exact mechanism by which CURMs exert antioxidant and anticancer effect is not elucidated in the present work. Furthermore, other functionalities of marinosomes relevant to biopharmaceutical field like controlled release, solubilizing other hydrophobic drugs, combination therapy and *in vivo* anticancer activity are future aspects of study.

3.6. References

Aadinath, W., Bhushani, A., Anandharamakrishnan, C., 2016. Synergistic radical scavenging potency of curcumin-in-β-cyclodextrin-in- nanomagnetoliposomes, Mater Sci. Eng. C Mater Biol. Appl. 64, 293–302

Ahmed, K., Li, Y., McClements, D.J., Xiao, H., 2012. Nanoemulsion- and emulsion-based delivery systems for curcumin: Encapsulation and release properties. Food Chem. 132, 799–807.

Alaarg, A., Ordan, N., Verhoef, J., Metselaar, J., Storm, G., Kok, R., 2016. Docosahexaenoic acid liposomes for targeting chronic inflammatory diseases and cancer: an in vitro assessment. Int. J. Nanomed. 11, 5027–5040.

Anand, P., Kunnumakkara, A.B., Newman, R.A., Aggarwal, B.B., 2007. Bioavailability of curcumin: Problems and promises. Mol. Pharm. 4, 807–818.

Anuchapreeda, S., Fukumori, Y., Okonogi, S., Ichikawa, H., 2011. Preparation of lipid nanoemulsions incorporating curcumin for cancer therapy. J. Nanotech. 2012. https://doi.org/10.1155/2012/270383

Applegate, K.R., Glomset, J. a, 1986. Computer-based modeling of the conformation and packing properties of docosahexaenoic acid. J. Lipid. Res. 27, 658–680.

Balasubramanyam, K., Varier, R.A., Altaf, M., Swaminathan, V., Siddappa, N.B., Ranga, U., Kundu, T.K., 2004. Curcumin, a novel p300/CREB-binding protein-specific inhibitor of acetyltransferase, represses the acetylation of histone/nonhistone proteins and histone acetyltransferase-dependent chromatin transcription. J. Biol. Chem. 279, 51163–51171.

Balkwill, F., Mantovani, A., 2001. Inflammation and cancer: back to Virchow? Lancet 357, 539–545.

Began, G., Sudharshan, E., Udaya Sankar, K., Rao, A., 1999. Interaction of curcumin with phosphatidylcholine: A spectrofluorometric study. J. Agric. Food Chem. 47, 4992–4997.

Bharti, A.C., Donato, N., Aggarwal, B.B., 2003. Curcumin (diferuloylmethane) inhibits constitutive and IL-6-Inducible STAT3 phosphorylation in human multiple myeloma cells. J. Immunol. 171, 3863–3871.

Bierhaus, A., Zhang, Y., Quehenberger, P., Luther, T., Haase, M., Müller, M., Mackman, N., Ziegler, R., Nawroth, P.., 1997. The dietary pigment curcumin reduces endothelial tissue factor gene expression by inhibiting binding of AP-1 to the DNA and activation of NF-kappa B. Thromb. Haemost. 77, 772–782.

Bisht, S., Feldmann, G., Soni, S., Ravi, R., Karikar, C., Maitra, A., Maitra, A., 2007. Polymeric nanoparticle-encapsulated curcumin ("nanocurcumin"): a novel strategy for human cancer therapy. J. Nanobiotechnol. 5, 3.

Blanckaert, V., Ulmann, L., Mimouni, V., Antol, J., Brancquart, L., Chénais, B., 2010. Docosahexaenoic acid intake decreases proliferation, increases apoptosis and decreases the invasive potential of the human breast carcinoma cell line MDA-MB-231. Int. J. Oncol. 36, 737–742.

Bradley, M.O., Webb, N.L., Anthony, F.H., Devanesan, P., Witman, P. a, Hemamalini, S., Chander, M.C., Baker, S.D., He, L., Horwitz, S.B., Swindell, C.S., 2001. Tumor targeting by covalent conjugation of a natural fatty acid to paclitaxel. Clin. Cancer Res. 7, 3229–3238.

Buszello, K., Harnisch, S., Müller, R., Müller, B., 2000. The influence of alkali fatty acids on the properties and the stability of parenteral O/W emulsions modified with solutol HS 15. Eur. J. Pharm. Biopharm. 49, 143–149.

Calder, P.C., 2012. Long-chain fatty acids and inflammation. Proc. Nutr. Soc. 71, 284–289.

Carmeliet, P., 2003. Angiogenesis in health and disease. Nat. Med. 9, 653–660.

Castro-Gómez, M.P., Holgado, F., Rodríguez-Alcalá, L.M., Montero, O., Fontecha, J., 2015. Comprehensive study of the lipid classes of krill oil by fractionation and identification of triacylglycerols, diacylglycerols, and phospholipid molecular species by using UPLC/QToF-MS. Food Anal. Method. 8, 2568–2580.

Chen, X., Zou, L.Q., Niu, J., Liu, W., Peng, S.F., Liu, C.M., 2015. The stability, sustained release and cellular antioxidant activity of curcumin nanoliposomes. Molecules 20, 14293–14311.

Cho, S.Y., Joo, D.S., Choi, H.G., Naraand, E., Miyashita, K., 2001. Oxidative stability of lipids from squid tissues. Fish. Sci. 67, 738–743.

Choudhury, D., Ganguli, A., Dastidar, D.G., Acharya, B.R., Das, A., Chakrabarti, G., 2013. Apigenin shows synergistic anticancer activity with curcumin by binding at different sites of tubulin. Biochimie 95, 1297–1309.

Cohen, A.W., Hnasko, R., Schubert, W., Lisanti, M.P., 2004. Role of caveolae and caveolins in health and disease. Physiol. Rev. 84, 1341–1379.

D'Eliseo, D., Velotti, F., 2016. Omega-3 Fatty Acids and Cancer Cell Cytotoxicity: Implications for Multi-Targeted Cancer Therapy. J. Clin. Med. 5, 15.

Das, U.N., 2006. Biological significance of essential fatty acids. The Journal of the Assoc. Physician. India 54, 309–319.

Desai, K., 2010. Curcumin cyclodextrin combination for preventing or treating various diseases. US Patent Application US20100179103.

Neptune Technologies & Bioressources , 2001. Natural phospholipids of marine origin containing flavonoids and polyunsaturated phospholipids and their uses. European Patent EP1417211 A2.

Feng, J.-Y., Liu, Z.-Q., 2009. Phenolic and enolic hydroxyl groups in curcumin: Which plays the major role in scavenging radicals? J. Agric. Food Chem. 57, 11041–11046.

Gerber, M., 2012. Omega-3 fatty acids and cancers: a systematic update review of epidemiological studies. Br. J. Nutr. 107, S228–S239.

Geusens, P., Wouters, C., Nijs, J., 1994. Long□term effect of omega□3 fatty acid supplementation in active rheumatoid arthritis. Arthritis Rheum. 37, 824–829.

Grit, M., Zuidam, N.J., Underberg, W.J.M., Crommelin, D.J.A., 1993. Hydrolysis of partially saturated egg phosphatidylcholine in aqueous liposome dispersions and the effect of cholesterol incorporation on hydrolysis kinetics. J. Pharm. Pharmacol. 45, 490–495.

Hong, J., Bose, M., Ju, J., Ryu, J.H., Chen, X., Sang, S., Lee, M.J., Yang, C.S., 2004. Modulation of arachidonic acid metabolism by curcumin and related β-diketone derivatives: Effects on cytosolic phospholipase A2, cyclooxygenases and 5-lipoxygenase. Carcinogenesis. 25, 1671–1679.

Iigo, M., Nakagawa, T., Ishikawa, C., Iwahori, Y., Asamoto, M., Yazawa, K., Araki, E., Tsuda, H., 1997. Inhibitory effects of docosahexaenoic acid on colon carcinoma 26 metastasis to the lung. Br. J. Cancer 75, 650–655.

Jin, H.-H., Lu, Q. & Jiang, J.-G, 2016. Curcumin liposomes prepared with milk fat globule membrane phospholipids and soybean lecithin. J. Dairy. Sci. 99, 1780–1790.

Kuhn, D., A., Vanhecke, D., Michen, B., Blank, F., Gehr, P., Petri-Fink, A., 2014. Different endocytotic uptake mechanisms for nanoparticles in epithelial cells and macrophages. Beilstein J. Nanotechnol. 5, 1625–1636.

Kuznetsova, L., Chen, J., Sun, L., Wu, X., Pepe, A., Veith, J.M., Pera, P., Bernacki, R.J., Ojima, I., 2006. Syntheses and evaluation of novel fatty acid-second-generation taxoid conjugates as promising anticancer agents. Bioorg. Med. Chem. Lett 16, 974–977.

Li, L., Braiteh, F., Kurzrock, R., 2005. Liposome-encapsulated curcumin: in vitro and in vivo effects on proliferation, apoptosis, signaling, and angiogenesis. Cancer 104, 1322–1331.

Lu, F., Nielsen, N., Timm-Heinrich, M., Acobsen, C., 2011. Oxidative stability of marine phospholipids in the liposomal form and their applications. Lipids 46, 3–23.

Lu, F.S.H., Nielsen, N.S., Baron, C.P., Jensen, L.H.S., Jacobsen, C., 2012. Physico-chemical properties of marine phospholipid emulsions. J. Am. Oil Chem.' Soc. 89, 2011–2024.

Ma, D.W.L., Seo, J., Switzer, K.C., Fan, Y.Y., McMurray, D.N., Lupton, J.R., Chapkin, R.S., 2004. n-3 PUFA and membrane microdomains: A new frontier in bioactive lipid research. J. Nutr. Biochem. 15, 700–706.

Ma, Z., Haddadi, A., Molavi, O., Lavasanifar, A., Lai, R., Samuel, J., 2007. Micelles of poly(ethylene oxide)-b-poly(e-caprolactone) as vehicles for the solubilization, stabilization, and controlled delivery of curcumin. J. Biomed. Mater Res. A 86, 300–310.

MacDonald, R.C., MacDonald, R.I., Menco, B.P.M., Takeshita, K., Subbarao, N.K., Hu, L., 1991. Small-volume extrusion apparatus for preparation of large, unilamellar vesicles. Biochim. Biophys. Acta 1061, 297–303.

Madri, J., Bell, L., Marx, M., Merwin, J., Basson, C., Prinz, C., 1991. Effects of soluble factors and extracellular matrix components on vascular cell behavior in vitro and in vivo: Models of de-endothelialization and repair. J. Cell Biochem. 45, 123–130.

Maiti, K., Mukherjee, K., Gantait, A., Saha, B.P., Mukherjee, P.K., 2007. Curcumin-phospholipid complex: Preparation, therapeutic evaluation and pharmacokinetic study in rats. Int. J. Pharm. 330, 155–163.

Mehta, H.J., Patel, V., Sadikot, R.T., 2014. Curcumin and lung cancer—a review. Targeted Oncol. 9, 295–310.

Merendino, N., Costantini, L., Manzi, L., Molinari, R., D'Eliseo, D., Velotti, F., 2013. Dietary ω-3 polyunsaturated fatty acid DHA: A potential adjuvant in the treatment of cancer. Biomed. Res. Int.

Mohanty, C., Acharya, S., Mohanty, A.K., Dilnawaz, F., Sahoo, S.K., 2010. Curcumin-encapsulated MePEG/PCL diblock copolymeric micelles: a novel controlled delivery vehicle for cancer therapy. Nanomed. 5, 433–449.

Moussaoui, N., Cansell, M., Denizot, A, 2002. Marinosomes®, marine lipid-based liposomes: Physical characterization and potential application in cosmetics. Int. J. Pharm. 242, 361–365.

National Comprehensive Cancer Network Guideline 2018 https://www.nccn.org/patients/guidelines/lung-nsclc/index.html. (accessed 5 December 2017).

Nicklisch, S.C.T., Waite, J.H., 2014. Optimized DPPH assay in a detergent-based buffer system for measuring antioxidant activity of proteins. MethodsX 1, 233–238.

Pendurthi, U., Rao, L., 2000. Suppression of transcription factor Egr-1 by curcumin. Thromb. Res. 97, 179–189.

Peng, J., Larondelle, Y., Pham, D., Ackman, R.G., Rollin, X., 2003. Polyunsaturated fatty acid profiles of whole body phospholipids and triacylglycerols in anadromous and landlocked Atlantic salmon (*Salmo salar L.*) fry. Comp. Biochem. Physiol. B Biochem. Mol. Biol. 134, 335–348.

Prior, R., Wu, X., Schaich, K., 2005. Standardized methods for the determination of antioxidant capacity and phenolics in foods and dietary supplements. J. Agric. Food Chem. 53, 4290–4302.

Ross, J.S., Stagliano, N.E., Donovan, M.J., Breitbart, R.E., Ginsburg, G.S., 2001. Atherosclerosis and cancer: common molecular pathways of disease development and progression. Annals NY Acad. Sci. 947, 271–273.

Saiz, L., Klein, M.L., 2001. Structural properties of a highly polyunsaturated lipid bilayer from molecular dynamics simulations. Biophys J. 81, 204–16.

Sauer, L. a, Dauchy, R.T., 1992. The effect of omega-6 and omega-3 fatty acids on 3H-thymidine incorporation in hepatoma 7288CTC perfused in situ. Br. J. Cancer 66, 297–303.

Sawada, N., Inoue, M., Iwasaki, M., Sasazuki, S., Shimazu, T., Yamaji, T., Takachi, R., Tanaka, Y., Mizokami, M., Tsugane, S., 2012. Consumption of n-3 fatty acids and fish reduces risk of hepatocellular carcinoma. Gastroenterol. 142, 1468–1475.

Schmidt, E.B., Varming, K., Pedersen, J.O., Lervang, H.H., Grunnet, N., Jersild, C., Dyerberg, J., 1992. Long-term supplementation with n-3 fatty acids, II: Effect on neutrophil and monocyte chemotaxis. Scand. J. Clin. Lab. Invest. 52, 229–36.

Schmitz, G., Ecker, J., 2008. The opposing effects of n-3 and n-6 fatty acids. Progress Lipid Res. 47, 147–155.

Sharma, O.P., Bhat, T.K., 2009. DPPH antioxidant assay revisited. Food Chem. 113, 1202–1205.

Shishodia, S., Potdar, P., Gairola, C.G., Aggarwal, B.B., 2003. Curcumin (diferuloylmethane) down-regulates cigarette smoke-induced NFκB activation through inhibition of IκBα kinase in human lung epithelial cells: Correlation with suppression of COX-2, MMP-9 and cyclin D1. Carcinogenesis 24, 1269–1279.

Sou, K., Inenaga, S., Takeoka, S., Tsuchida, E., 2008. Loading of curcumin into macrophages using lipid-based nanoparticles. Int. J. Pharm. 352, 287–293.

Szymczak, M., Murray, M., Petrovic, N., Dc, W., Szymczak, M., Murray, M., Petrovic, N., 2008. Modulation of angiogenesis by ω -3 polyunsaturated fatty acids is mediated by cyclooxygenases. Blood. 111, 3514–3521.

Tagami, T., Imao, Y., Ito, S., Nakada, A., Ozeki, T., 2014. Simple and effective preparation of nano-pulverized curcumin by femtosecond laser ablation and the cytotoxic effect on C6 rat glioma cells in vitro. Int. J. Pharm. 468, 91–96.

Tagami, T., Kubota, M., Ozeki, T., 2015. Effective remote loading of doxorubicin into DPPC/Poloxamer 188 hybrid liposome to retain thermosensitive property and the assessment of carrier-based acute cytotoxicity for pulmonary administration. J. Pharm. Sci. 104, 3824–3832.

Thaloor, D., Singh, A.K., Sidhu, G.S., Prasad, P. V, Kleinman, H.K., Maheshwari, R.K., 1998. Inhibition of angiogenic differentiation of human umbilical vein endothelial cells by curcumin. Cell Growth Differ. 9, 305–312.

Vaughan, V.C., Hassing, M.-R., Lewandowski, P.A., 2013. Marine polyunsaturated fatty acids and cancer therapy. Br J Cancer 108, 486–492.

Villaño, D., Fernández-Pachón, M.S., Moyá, M.L., Troncoso, A.M., García-Parrilla, M.C., 2007. Radical scavenging ability of polyphenolic compounds towards DPPH free radical. Talanta 71, 230–235.

Voigt, J., Christensen, J., Shastri, V.P., 2014. Differential uptake of nanoparticles by endothelial cells through polyelectrolytes with affinity for caveolae. Proc Natl Acad Sci U S A 111, 2942–2947.

Wijendran, V., Huang, M.-C., Diau, G.-Y., Boehm, G., Nathanielsz, P.W., Brenna, J.T., 2002. Efficacy of dietary arachidonic acid provided as triglyceride or phospholipid as substrates for brain arachidonic acid accretion in baboon neonates. Pediatr. Res. 51, 265–72.

Winther, B., Hoem, N., Berge, K., Reubsaet, L., 2011. Elucidation of phosphatidylcholine composition in krill oil extracted from *Euphausia superba*. Lipids 46, 25–36.

Yin, Y., Sui, C., Meng, F., Ma, P., Jiang, Y., 2017. The omega-3 polyunsaturated fatty acid docosahexaenoic acid inhibits proliferation and progression of non-small cell lung cancer cells through the reactive oxygen species-mediated inactivation of the PI3K /Akt pathway. Lipids Health Dis. 16, 87.

Acknowledgment

First of all, Thanks so much for ALLAH, the real creator for the universe and my god, for his divine care that enabled me to accomplish this work.

Completing a PhD is truly looking like a marathon event. Without a doubt, I would not have been able to complete this PhD, if I didn't receive the aid and support from a lot of people over the past three years.

First of all, I express my deeply and sincerely gratitude to my Professor Tetsuya Ozeki. Prof. Ozeki, I would like to express my profound gratitude to you for your excellent guidance, support and invaluable suggestions. You have supported me with promptness, patience and encouragement in all times, especially during difficulties. You didn't only teach me lessons in science but also a lot of lessons in life that I have learned from you even by talking with you or seeing your actions.

I would like to express my profound gratitude to Prof. Tatsukai Tagami. Dear Prof. Tagami, I’m so gratefull for your excellent supervision during my doctor period and for the time you spent reading and commenting my articles and thesis. Your ideas and suggestions have helped me to improve my work. Your hard work, patience and kindness set an example, which I appreciate from my heart.

I would like to express my thankfulness and gratefulness to Dr. Noriko Ogawa, Dr. Chisato Takahashi and Prof. Hiromitsu Yamamoto (Aichi-Gakuin University) for giving me the chance for some measurements in their lab.

Many thanks are also for Dr. Takayuki Terukina for his useful discussions, support and encouragement during his two years stay at this Lab. I express my deep thankfulness for Dr. Takeuchi for his help and support.

I wish to extend my thanks to all the members of Drug Delivery and Nanopharmaceutices department for the non-step support and feedback they supported me during my doctor journey. Their friendship, useful discussions and technical assistance especially at the beginning of this work have helped me a lot to complete my work. Among them, I am deeply thankful to Mr. Fuse, Mr. Ando, Ms. Taki, and Mr. Tane.

I also wish to express my thankfulness for my dear friend, Dr. Eman Mohamed, for her spiritual support and scientific discussion. My gratefulness for all my friends who were always beside me during this journey.

My endless gratitude goes to my parents for their extreme attention to my education and their extreme emotional support and encouragement. Also thanks so much for my brothers and sisters for their invocations and encouragement.

Special thanks for my sincere husband for his endless support and encouragement. Also thanks for my little children, Sama, EL Baraa and Hamza, for their strong support and company.

I am expressing my gratefulness and complete loyalty to my home country Egypt and my gratefulness to the beloved country Japan for the great hospitality and the scholarship, Rotary Yoneyama Memorial scholarship that enabled me to accomplish this work.